

Si–H Bond Activation by $(\text{Ph}_3\text{P})_2\text{Pt}(\eta^2\text{-C}_2\text{H}_4)$ in Dihydrosilicon Tricycles that Also Contain O and N Heteroatoms

Janet Braddock-Wilking,* Joyce Y. Corey, Lisa M. French, Eunwoo Choi, Victoria J. Speedie, Michael F. Rutherford, Shu Yao, Huan Xu, and Nigam P. Rath

Department of Chemistry and Biochemistry, University of Missouri–St. Louis, St. Louis, Missouri 63121

Received May 8, 2006

Several tricyclic phenoxasilin and phenazasilin heterocycles were synthesized from the corresponding 2,2'-dilithio-diphenyl ether or diphenyl amine precursor and silicon tetrachloride (or trichlorosilane) followed by reduction with lithium aluminum hydride [H_2SiAr_2 : $\text{Ar}_2 = \text{C}_{12}\text{H}_8\text{O}$ (**1**); $\text{Ar}_2 = \text{C}_{14}\text{H}_{12}\text{O}$ (**2**); $\text{Ar}_2 = \text{C}_{13}\text{H}_{11}\text{N}$ (**3**); $\text{Ar}_2 = \text{C}_{15}\text{H}_{15}\text{N}$ (**4**); $\text{Ar}_2 = \text{C}_{13}\text{H}_9\text{Br}_2\text{N}$ (**5**)]. The reactivity of hydrosilanes **1–5** with $(\text{Ph}_3\text{P})_2\text{Pt}(\eta^2\text{-C}_2\text{H}_4)$ (**6**) was investigated. At room temperature, mononuclear complexes, $(\text{Ph}_3\text{P})_2\text{Pt}(\text{H})(\text{SiAr}_2\text{H})$ and $(\text{Ph}_3\text{P})_2\text{Pt}(\text{SiAr}_2\text{H})_2$, were generally observed by NMR spectroscopy but were too reactive or unstable to isolate. Dinuclear and in some cases trinuclear Pt–Si-containing complexes were observed as the major products from the reactions. Symmetrical dinuclear complexes, $[(\text{Ph}_3\text{P})\text{Pt}(\mu\text{-}\eta^2\text{-H-SiAr}_2)]_2$ (**8** and **22**, respectively), were produced from the reaction of **1** or **3** with **6**. In contrast, reaction of silane **2** with **6** produced a trinuclear complex, $[(\text{Ph}_3\text{P})\text{Pt}(\mu\text{-SiAr}_2)]_3$ (**16**), as the major product. However, reaction of **4** or **5** with complex **6** produced an unsymmetrical dinuclear complex, $[(\text{Ph}_3\text{P})_2\text{Pt}(\text{H})(\mu\text{-SiAr}_2)(\mu\text{-}\eta^2\text{-H-SiAr}_2)\text{Pt}(\text{PPh}_3)]$ (**26** and **30**, respectively), as the major component. The molecular structures of a symmetrical (**22**) and unsymmetrical dinuclear (**30**) complex as well as a trinuclear (**16**) complex were determined by X-ray crystallography.

Introduction

Hydrosilanes are known to react with a variety of transition-metal precursors in Si–H bond activation processes to generate new complexes containing a TM–Si bond.^{1,2} Most early transition-metal complexes are believed to interact with Si–H bonds through a σ -bond metathesis pathway, whereas late metals probably proceed through an oxidative-addition route.¹ A variety of Si–TM products can be generated depending upon the type of hydrosilane and metal precursor used. The most studied reactions involve a tertiary hydrosilane (HSiR_3) with simple organic groups where the expected product resulting from formal insertion of the metal into the Si–H bond gives a complex with the general formula $\text{L}_n\text{M}(\text{H})(\text{SiR}_3)$. However, with secondary (R_2SiH_2) and primary (RSiH_3) hydrosilanes, additional Si–H bonds provide further potential sites of reactivity not available with tertiary precursors. In general, these precursors can provide mono-, di-, and multinuclear complexes containing M–Si bonds with terminal and/or bridging silicon and hydride ligands.^{1,2}

In the early 1970s the Pt(0) complex $(\text{Ph}_3\text{P})_2\text{Pt}(\eta^2\text{-C}_2\text{H}_4)$ was found to react with diphenylsilane, Ph_2SiH_2 , as well as a number of triarylsilanes to provide mononuclear complexes through

oxidative addition of an Si–H bond to give, for example, $(\text{Ph}_3\text{P})_2\text{Pt}(\text{H})(\text{SiPh}_2\text{H})$.³ Our recent studies of $(\text{Ph}_3\text{P})_2\text{Pt}(\eta^2\text{-C}_2\text{H}_4)$ with Ph_2SiH_2 and silafluorene ($\text{H}_2\text{SiC}_{12}\text{H}_8$) showed that mononuclear and dinuclear complexes are formed, but with silafluorene an unexpected trinuclear complex was also produced.⁴ Our studies have been extended to the study of the reaction of phenoxasilin and phenazasilin rings containing two exocyclic Si–H bonds, and herein we report the synthesis, characterization, and reactivity of these ring systems with $(\text{Ph}_3\text{P})_2\text{Pt}(\eta^2\text{-C}_2\text{H}_4)$.

Results

Preparation and Characterization of Silicon Heterocycles.

The tricyclic silicon ring systems in the current study all contain silicon and either an oxygen or a nitrogen atom in the central six-membered ring (Scheme 1). There were two general synthetic strategies that were used to prepare the heterocycles **1–5** (Scheme 1). The presence of the heteroatoms in the starting diphenyl ethers or amines enabled the direct lithiation at the site *ortho* to the heteroatom in the initial, generally commercially available, hydrocarbon precursor. Alternatively, the appropriate *o,o'*-dibromide precursor could be used to prepare the desired dilithio reagent. The dibromide precursor has the disadvantage that its preparation involves additional reaction steps and purification can be complicated due to the difficulty of controlling the bromination reaction sequence, which results in several

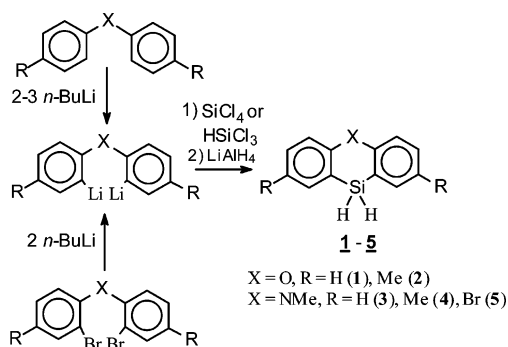
* To whom correspondence should be addressed. E-mail: wilkingj@umsl.edu. Fax: (314) 516-5342. Tel: (314) 516-6436.

(1) Corey, J. Y.; Braddock-Wilking, J. *Chem. Rev.* **1999**, *99*, 175.
 (2) (a) Aylett, B. J. *Adv. Inorg. Chem. Radiochem.* **1982**, *25*, 1. (b) Tilley, T. D. Transition-Metal Silyl Derivatives. In *The Chemistry of Organic Silicon Compounds*; Patai, S., Rappoport, Z., Eds.; John Wiley and Sons: New York, 1989; p 1416. (c) Schubert, U. *Adv. Organomet. Chem.* **1990**, *30*, 151. (d) Tilley, T. D. Transition-Metal Silyl Derivatives. In *The Silicon Heteroatom Bond*; Patai, S., Rappoport, Z., Eds.; John Wiley and Sons: New York, 1991; p 245. (e) Schubert, U. *Transition Met. Chem.* **1991**, *16*, 126. (f) Tobita, H.; Ogino, H. *Adv. Organomet. Chem.* **1998**, *42*, 223. (g) Eisen, M. S. Transition-Metal Silyl Complexes. In *The Chemistry of Organic Silicon Compounds*; 1998; Vol. 2 (Part 3), p 2037. (h) Braunstein, P.; Boag, N. M. *Angew. Chem., Int. Ed.* **2001**, *40*, 2427. (i) Nikonov, G. *Adv. Organomet. Chem.* **2005**, *53*, 217.

(3) (a) Eaborn, C.; Ratcliff, B.; Pidcock, A. *J. Organomet. Chem.* **1974**, *65*, 181. (b) Eaborn, C.; Pidcock, A.; Ratcliff, B. *J. Organomet. Chem.* **1972**, *43*, C5.

(4) (a) Braddock-Wilking, J.; Corey, J. Y.; Trankler, K. A.; Xu, H.; French, L. M.; Praingam, N.; White, C.; Rath, N. P. *Organometallics* **2006**, *25*, 2859. (b) Braddock-Wilking, J.; Corey, J. Y.; Trankler, K. A.; Dill, K. M.; French, L. M.; Rath, N. P. *Organometallics* **2004**, *23*, 4576. (c) Braddock-Wilking, J.; Corey, J. Y.; Dill, K. M.; Rath, N. P. *Organometallics* **2002**, *21*, 5467.

Scheme 1



products containing varying numbers of bromine substituents.⁵ The two sequences converge at the dilithio stage; therefore a one-pot synthesis can be performed from either direction followed by quenching with either trichlorosilane or silicon tetrachloride. The resulting dichloro-substituted silicon heterocycle (or chloro(hydrido)silicon heterocycle from HSiCl_3) need not be isolated and can be reduced with lithium aluminum hydride to give the secondary hydrosilanes (**1–4**). The bromo-substituted phenazasiline **5** was prepared according to the literature procedure utilizing the precursor 2,2',4,4'-tetrabromo-*N*-methylidiphenylamine.⁵ Despite the anticipated ease of preparing substituted ring systems, incorporation of groups on the aromatic rings is generally difficult and can require multiple steps.⁶ The phenoxasilin and phenazasiline rings **2**, **3**, and **4** are additional examples of these ring systems containing two exocyclic hydride substituents at the silicon center.

Compound **1** was prepared by a modified literature procedure (Scheme 1).^{8,9} The dilithio reagent was prepared in THF at low temperature by metalation of diphenyl ether with 3 equiv of butyllithium followed by quenching with SiCl_4 and then reduction with lithium aluminum hydride to afford **1** as a viscous, pungent-smelling liquid in approximately 20% yield. The metalation of diphenyl ether in the presence of TMEDA has also been reported;¹⁰ however, attempts to prepare **1** using activation by TMEDA failed. When the dilithio reagent was quenched with $\text{Si}(\text{OMe})_4$ instead of SiCl_4 before reduction with LiAlH_4 , formation of **1** was not observed. Compound **2** was prepared in 11% isolated yield by a route similar to that shown in Scheme 1 starting from *p*-tolyl ether.

The initial attempts to synthesize 10,10-dihydro-5-methylphenazasiline, **3**, began with the multistep preparation of the dibromo precursor *o,o'*-dibromophenyl-*N*-methylamine.¹¹ Later, a modified procedure was followed starting from commercial *N*-methylidiphenylamine.¹² The latter reaction involved meta-

lation with butyllithium in the presence of TMEDA followed by ring closure with silicon tetrachloride¹² and reduction with LiAlH_4 (eq 2). The product **3** was obtained in 59% yield (GC), but the several required purification steps provided only 4% isolated yield as a tan solid.

The 2,5,8-trimethyl-10,10-dihydrophenazasiline, **4**, and its deuterium analogue 2,5,8-trimethyl-10,10-dideuterophenazasiline, **4-d₂**, were prepared from a sequence starting from the reaction of bis(2-bromo-4-methylphenyl)-*N*-methylamine with *n*-BuLi at low temperature. The corresponding dilithio reagent was then reacted with trichlorosilane followed by addition of LiAlH_4 (or LiAlD_4) (Scheme 1). The products **4** and **4-d₂** were isolated in 42 and 24% yield, respectively.

All of the silicon heterocycles **1–5** in this study exhibited Si-H resonances in the expected region near 5 ppm in the ^1H NMR spectrum. The $^{29}\text{Si}\{^1\text{H}\}$ signals for **1–5** were observed between -54 and -64 ppm, in the region normally found for secondary arylhydrosilanes.¹³ The presence of the Si-H unit in **1–5** was also confirmed by IR spectroscopy, where strong Si-H stretching bands were observed near 2100 cm^{-1} .¹⁴

Reactivity Studies of Silicon Heterocycles 1–5 with $(\text{Ph}_3\text{P})_2\text{Pt}(\eta^2\text{-C}_2\text{H}_4)$ (6**).** The Pt(0) complex $(\text{Ph}_3\text{P})_2\text{Pt}(\eta^2\text{-C}_2\text{H}_4)$ (**6**) was found to react readily with all of the heterocycles (**1–5**) at low temperature as well as room temperature and above. The reactions were monitored by NMR spectroscopy, and the experiments with each heterocycle are described in subsequent paragraphs. Key NMR spectroscopic data for the major products observed are listed in Table 1. Additional characterization data for the complexes formed in the following reactions are provided in the Experimental Section.

Reaction of 10,10-Dihydrophenoxasilin (1**) with $(\text{Ph}_3\text{P})_2\text{Pt}(\eta^2\text{-C}_2\text{H}_4)$ (**6**).** The unsubstituted phenoxasilin **1** reacted with complex **6** immediately upon mixing at room temperature, as evidenced by vigorous gas evolution of C_2H_4 and H_2 and observation of resonances for these compounds by ^1H NMR spectroscopy. The major product isolated from the reaction was the symmetrical dinuclear complex $[(\text{Ph}_3\text{P})\text{Pt}(\mu\text{-}\eta^2\text{-H-SiC}_2\text{H}_5\text{O})_2]$ (**8**) (Scheme 2), which precipitated in the NMR tube within 30 min after mixing and was isolated as a sparingly soluble golden-yellow solid in 71% yield. The ^1H NMR spectrum for isolated complex **8** in CD_2Cl_2 exhibited a resonance at 3.25 ppm for the bridging ($\text{Pt}\cdots\text{H}\cdots\text{Si}$) hydride with both one- and two-bond couplings to Pt. The $^{31}\text{P}\{^1\text{H}\}$ NMR spectrum showed a resonance centered at 36 ppm for **8** with the expected pattern of an AA'XX' spin system similar to that which was observed for the related symmetrical dinuclear Pt complexes previously reported.^{15–17}

When the reaction was performed at room temperature and monitored by ^1H NMR spectroscopy, the data collected within

(5) Corey, J. Y.; John, C. J.; Ohmstead, M. C.; Chang, L. S. *J. Organomet. Chem.* **1986**, 304, 93.

(6) See for example the preparation of 2,2'-dibromo-4,4'-dimethylbiphenyl: (a) Gattermann, L. *Ber.* **1890**, 23, 1219. (b) Niementowski. *Ber.* **1901**, 34, 3327. (c) Schwechten, H.-W. *Ber.* **1932**, 65, 1605. (d) We thank Professor Peter P. Gaspar of Washington University for assistance in translating the Experimental Sections in refs 6a–c.

(7) Reikhsfel'd, V. O.; Nesterova, S. V.; Skvortsov, N. K.; Kupce, E.; Lukevics, E. *Z. Obshch. Khim.* **1986**, 56, 1306.

(8) Kreisel, G.; Rudolph, G.; Schulze, D. K. W.; Poppitz, W. *Monatsch. Chem.* **1992**, 123, 1153.

(9) For additional reports on the preparation of related phenoxa ring systems see: (a) Kostenko, N. L.; Nesterova, S. V.; Toldov, S. V.; Skvortsov, N. K.; Reikhsfel'd, V. O. *Zh. Obshch. Khim.* **1987**, 57, 716. (b) Chang, V. H. T.; Corey, J. Y. *J. Organomet. Chem.* **1980**, 190, 217. (c) Reikhsfel'd, V. O.; Yakovlev, I. P.; Saratov, I. E. *Zh. Obshch. Khim.* **1979**, 49, 776. (d) Meinema, H. A. J. *Organomet. Chem.* **1973**, 63, 243. (e) Gilman, H.; Trepka, W. J. *J. Org. Chem.* **1962**, 27, 1418. (f) Oita, K.; Gilman, H. *J. Am. Chem. Soc.* **1957**, 79, 339.

(10) Fink, W. *Helv. Chim. Acta* **1973**, 56, 355.

(11) (a) Furniss, B. S.; Hannaford, A. J.; Smith, P. W. G.; Tatchell, A. R. *Textbook of Practical Organic Chemistry*, 5th ed.; Longman Scientific & Technical: Essex, England, 1989; p 1261. (b) Jones, E. R.; Mann, F. G. *J. Chem. Soc.* **1956**, 786. (c) Gilman, H.; Zuech, E. A. *J. Org. Chem.* **1961**, 26, 2013.

(12) Lee, M. E.; Cho, H. M.; Kim, C. H.; Ando, W. *Organometallics* **2001**, 20, 1472.

(13) Williams, E. A. NMR spectroscopy of Organosilicon Compounds. In *The Chemistry of Organic Silicon Compounds*; Patai, S., Rappoport, Z. Eds.; John Wiley and Sons: New York, 1989; p 511.

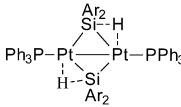
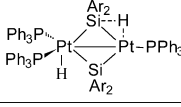
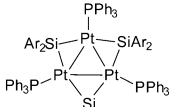
(14) Crews, P.; Rodríguez, J.; Jaspars, M. *Organic Structure Analysis*; Oxford University Press: New York, 1998; p 317.

(15) Braddock-Wilking, J.; Corey, J. Y.; White, C.; Xu, H.; Rath, N. P. *Organometallics* **2005**, 24, 4113.

(16) Tanabe, M.; Yamada, T.; Osakada, K. *Organometallics* **2003**, 22, 2190.

(17) Auburn, M.; Ciriano, M.; Howard, J. A. K.; Murray, M.; Pugh, N. J.; Spencer, J. L.; Stone, F. G. A.; Woodward, P. *J. Chem. Soc., Dalton Trans.* **1980**, 659.

Table 1. Comparison of Selected NMR Spectroscopic Data for Key Complexes in This Report^a

(Ph ₃ P) ₂ Pt ^H ₂ SiAr ₂ H	Selected ¹ H and ³¹ P{ ¹ H} NMR data
Ar ₂ = C ₁₂ H ₈ O 7 (223 K)	¹ H: δ 5.41 (m, SiH); -1.50 (dd, ¹ J _{PtH} = 973, ² J _{PtH} = 156, 16, PtH) ³¹ P: δ 34.2 (br s, ¹ J _{PtP} = 1788, trans to Si); 33.4 (br s, ¹ J _{PtP} = 2422)
Ar ₂ = C ₁₄ H ₁₂ O 12 (223 K)	¹ H: δ 5.59 (m, SiH); -1.48 (dd, ¹ J _{PtH} = 977, ² J _{PtH} = 154, 19, PtH) ³¹ P: δ 33.3 (br s, ¹ J _{PtP} = 1761, trans to Si); 33.2 (br s, ¹ J _{PtP} = 2439)
Ar ₂ = C ₁₃ H ₁₁ N 17 (223 K)	¹ H: δ 4.86 (m, SiH); -1.28 (dd, ¹ J _{PtH} = 988, ² J _{PtH} = 156, 20, PtH) ³¹ P: δ 36.6 (d, ¹ J _{PtP} = 1818, trans to Si); 35.2 (br s, ¹ J _{PtP} = 2447)
Ar ₂ = C ₁₅ H ₁₅ N 23 (223 K)	¹ H: δ 4.96 (m, SiH); -1.31 (dd, ¹ J _{PtH} = 996, ² J _{PtH} = 155, 21, PtH) ³¹ P: δ 35.7 (br s, ¹ J _{PtP} = 1798, trans to Si); 35.3 (br s, ¹ J _{PtP} = 2455)
Ar ₂ = C ₁₃ H ₉ Br ₂ N 28 (223 K)	¹ H: δ 4.65 (m, SiH); -1.77 (dd, ¹ J _{PtH} = 973, ² J _{PtH} = 156, 18, PtH) ³¹ P: δ 35.0 (br s, ¹ J _{PtP} = 1863); 33.6 (br s, ¹ J _{PtP} = 2417)
	
Ar ₂ = C ₁₂ H ₈ O 8 (300 K, CD ₂ Cl ₂) ^e	¹ H: δ 3.25 (s, ¹ J _{PtH} = 691, ² J _{PtH} = 136, Pt···H···Si) ³¹ P: δ 36.6 (s, ¹ J _{PtP} = 4369, ² J _{PtP} = 249, ³ J _{PP} = 59)
Ar ₂ = C ₁₅ H ₁₅ N 22 (300 K, CD ₂ Cl ₂)	¹ H: δ 2.36 (s, Pt···H···Si) ^b ³¹ P: δ 36.9 (s, ¹ J _{PtP} = 4349, ² J _{PtP} = 265, ³ J _{PP} = 60)
	
Ar ₂ = C ₁₄ H ₁₂ O 15 (223 K)	¹ H: δ 2.71 (br, Pt···H···Si) ^b ; -5.04 (br s, ¹ J _{PtH} = 544, PtH) ³¹ P: δ 30.3 (br s, ¹ J _{PtP} = 4081, ² J _{PtP} = 198); 20.3 (br s, ¹ J _{PtP} = 3504) ^c
Ar ₂ = C ₁₃ H ₁₁ N 20 (223 K)	¹ H: δ (Pt···H···Si) not located; -5.98 (br s, ¹ J _{PtH} = 570, PtH) ³¹ P: δ 30.7 (br s, ¹ J _{PtP} = 4174, ² J _{PtP} = 278); 18.6 (d, ¹ J _{PtP} = 3666) ^c
Ar ₂ = C ₁₅ H ₁₅ N 26 (223 K)	¹ H: δ (Pt···H···Si) not located; -6.06 (t, ¹ J _{PtH} = 565, ² J _{PtH} = 13, PtH) ³¹ P: δ 30.2 (t, ¹ J _{PtP} = 4058, ² J _{PtP} = 253, ³ J _{PP} = 28); 19.4 (d, 3682) ^c
Ar ₂ = C ₁₃ H ₉ Br ₂ N 30 (223 K) ^d	¹ H: δ 2.91 (d, ² J _{PtH} = 11, Pt···H···Si) ^b ; -6.34 (t, ¹ J _{PtH} = 564, ² J _{PtH} = 15, PtH) ³¹ P: δ 28.1 (t, ¹ J _{PtP} = 4032, ² J _{PtP} = 280, ³ J _{PP} = 28); 18.5 (d, ¹ J _{PtP} = 3710) ^c
	
Ar ₂ = C ₁₂ H ₈ O 11 (323 K) ^f	no hydrides ³¹ P: δ 68.3 (s, ¹ J _{PtP} = 3454, ² J _{PtP} = 466, ³ J _{PP} = 76)
Ar ₂ = C ₁₄ H ₁₂ O 16 (300 K) ^{g, h}	no hydrides ³¹ P: δ 68.7 (s, ¹ J _{PtP} = 3474, ² J _{PtP} = 466, ³ J _{PP} = 76)
Ar ₂ = C ₁₃ H ₁₁ N 21 (323 K) ⁱ	no hydrides ³¹ P: δ 66.4 (s, ¹ J _{PtP} = 3528, ² J _{PtP} = 491, ³ J _{PP} = 76)
Ar ₂ = C ₁₅ H ₁₅ N 27 (300 K)	no hydrides ³¹ P: δ 67.4 (s, ¹ J _{PtP} = 3495, ² J _{PtP} = 494, ³ J _{PP} = 76)
Ar ₂ = C ₁₃ H ₉ Br ₂ N 31 (300 K)	no hydrides ³¹ P: δ 65.1 (s) ^b

^a In C₇D₈ solution unless otherwise noted. Chemical shifts are given in ppm and coupling constants in Hz. Si–H coupling not resolved. ^b Pt satellites not resolved. ^c ²J_{PtP} not resolved. ^d ²⁹Si resonances located at 136 and 137 ppm by 2D ¹H–²⁹Si HMQC experiment. ^e ²⁹Si resonance located at 128 ppm by 2D ¹H–²⁹Si HMQC experiment. ^f ¹⁹⁵Pt{¹H} resonance observed at –4376 ppm as a multiplet. ^g ²⁹Si resonance observed at 239.6 ppm (s, ¹J_{PtSi} = 976). ^h ¹⁹⁵Pt{¹H} resonance observed at –4352 ppm as a multiplet. ⁱ ²⁹Si resonance observed at 254.6 ppm (s, ¹J_{PtSi} = 964).

10 min after mixing showed a broad terminal hydride signal near –2 ppm that was assigned to the Pt–H in **7**. In addition, two resonances were observed in the Si–H region (between 5.4 and 5.8 ppm) that were assigned to **7** and to the bis(silyl) platinum complex (Ph₃P)₂Pt(HSiC₁₂H₈O)₂ (**9**) (Scheme 2). The ³¹P{¹H} NMR spectrum also collected after 10 min exhibited an intense broad signal centered at 11 ppm as well as a sharp signal for **9** as the major resonances. No resolved signals for **7** or **8** were observed, but it is likely that the broad resonance at 11 ppm involved a fluxional process with one or both of these complexes. The mononuclear complexes **7** and **9** appear to be thermally unstable or highly reactive, and NMR signals for these components are observed only in the early stages of the reaction. A minor signal was also observed in the ³¹P NMR spectrum that was assigned to the siloxy complex (Ph₃P)₂Pt[(SiC₁₂H₈O)₂O] (**10**). Complex **10** was probably formed by the reaction of **9** with adventitious oxygen or water in the reaction vessel. We

and other researchers have reported the preparation of related platinum–disiloxy complexes previously.^{4a,18,19} After 6 days two additional minor signals were observed by ³¹P{¹H} NMR spectroscopy and were assigned to the presence of trace amounts of [(Ph₃P)Pt(μ-SiC₁₂H₈O)]₃ (**11**) and Pt(PPh₃)₄.²⁰ In this and other reactions described in this report, signals for OPh₃ and PPh₃ were observed in the ³¹P{¹H} NMR spectra.

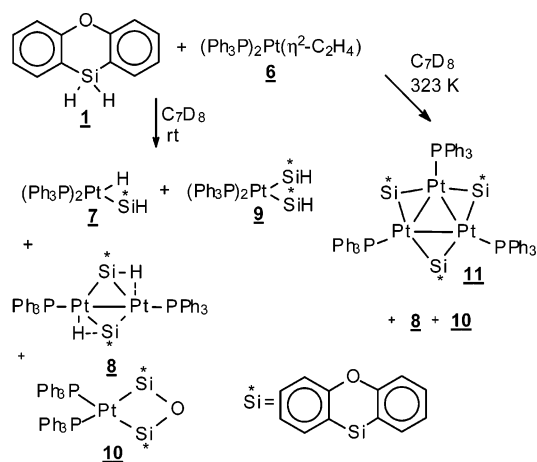
When the addition was carried out at low temperature (195 K) and monitored immediately by VT-NMR spectroscopy

(18) (a) Goikhman, R.; Karakuz, T.; Shimon, L. J. W.; Leitius, G.; Miltstein, D. *Can. J. Chem.* **2005**, *83*, 786. (b) Pham, E. K.; West, R. *J. Am. Chem. Soc.* **1989**, *111*, 7667. (c) Pham, E. K.; West, R. *Organometallics* **1990**, *9*, 1517. (d) Bell, L. G.; Gustavson, W. A.; Thanedar, S.; Curtis, M. D. *Organometallics* **1983**, *2*, 740. (e) Curtis, M. S.; Greene, J. J. *J. Am. Chem. Soc.* **1978**, *100*, 6362.

(19) Osakada, K.; Tanabe, M.; Tanase, T. *Angew. Chem., Int. Ed.* **2000**, *39*, 4053.

(20) Sen, A.; Halpern, J. *Inorg. Chem.* **1980**, *19*, 1073.

Scheme 2

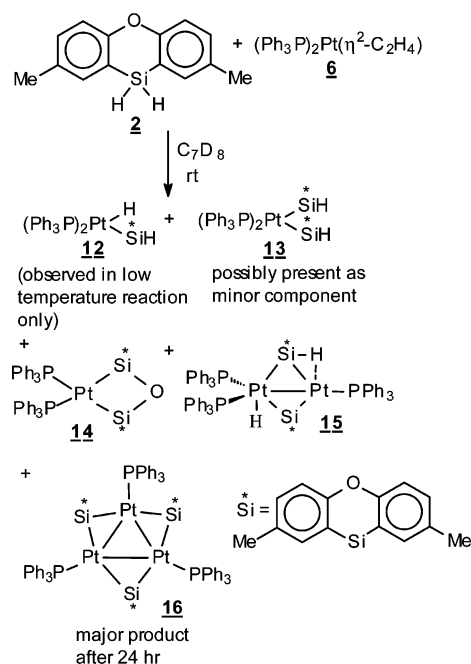


starting at 223 K, well-resolved sharp signals for **7** were observed in both the ^1H and $^{31}\text{P}\{^1\text{H}\}$ NMR spectra along with unreacted precursor **6**. The proton signals for the hydrides in **7** were observed at 5.4 ppm for the Si-H unit (multiplet overlapping with the signal for free C_2H_4) and at -1.5 ppm for the terminal Pt-H as a doublet of doublets with platinum satellites. The $^{31}\text{P}\{^1\text{H}\}$ NMR spectrum showed a broad singlet at 34 ppm for the phosphorus *trans* to silicon in **7** and a broad singlet at 33 ppm for the second phosphine *trans* to the hydride. No signals were observed for complex **9** in the low-temperature reaction. As the temperature was raised slowly to room temperature, the signals for **7** began to broaden significantly. When the temperature had reached 303 K (after 5 h), no resolved signals were observed for **6** or **7** in the ^1H NMR spectrum. The $^{31}\text{P}\{^1\text{H}\}$ NMR spectrum resembled that observed in the room-temperature addition, showing a broad peak centered at 20 ppm (range about 0–50 ppm) as the major signal. The latter signal remained broad even when the temperature was lowered to 223 K, but at 183 K sharp signals for $(\text{Ph}_3\text{P})_4\text{Pt}$ and PPh_3 were observed.²⁰

When the addition of **1** to **6** was performed at room temperature followed by immediate heating of the solution in the NMR magnet at 323 K, complex **8** was formed as the major product, but also observed by $^{31}\text{P}\{^1\text{H}\}$ NMR spectroscopy was the presence of the trinuclear complex **11**, $\text{Pt}(\text{PPh}_3)_4$ and PPh_3 (at low temperature), and complex **10** (Scheme 2).

Reaction of 2,8-Dimethyl-10,10-dihydrophenoxasilin (2) with $(\text{Ph}_3\text{P})_2\text{Pt}(\eta^2\text{-C}_2\text{H}_4)$ (6). The reaction of the tricyclic ring system **2** with the Pt(0) complex **6** at room temperature resulted in the formation of the unsymmetrical dinuclear complex $(\text{Ph}_3\text{P})_2(\text{H})\text{Pt}(\mu\text{-SiC}_8\text{H}_{12}\text{O})(\mu\text{-}\eta^2\text{-H-SiC}_8\text{H}_{12}\text{O})\text{Pt}(\text{PPh}_3)$ (**15**) as the major species (Scheme 3). The expected mononuclear complex **12**, analogous to **7**, appears to be reactive and was observed only in the low-temperature addition reaction. Complex **15** exhibits distinctive resonances in both the ^1H and $^{31}\text{P}\{^1\text{H}\}$ low-temperature NMR spectra due to the unsymmetrical environment at the Pt centers and dynamic behavior of the phosphine ligands on the NMR time scale. In the reaction solution at room temperature, a broad averaged resonance is observed at 0.4 ppm with flanking broad platinum satellites for the two hydrides in **15**. A broad peak was observed in the $^{31}\text{P}\{^1\text{H}\}$ NMR spectrum centered at 19 ppm and probably involved an exchange process between **15** and free PPh_3 in the solution.^{4a} Approximately 45 min after mixing, a signal for the triplatinum complex **16** was observed in the $^{31}\text{P}\{^1\text{H}\}$ NMR spectrum at 68.7 ppm as a central

Scheme 3



line flanked by a complex Pt satellite pattern due to the presence of several isotopomers containing ^{195}Pt .²¹

Upon cooling the reaction solution to 223 K, well-resolved signals for the dinuclear complex **15** were observed in addition to signals for **14**, **16**, and OPPh_3 . The $^{31}\text{P}\{^1\text{H}\}$ NMR spectrum displayed a triplet at 30.3 for the $\text{Pt}(\text{PPh}_3)$ unit and a doublet at 20.3 ppm for the $\text{Pt}(\text{PPh}_3)_2$ group in **15**, as well as a singlet at -5 ppm for PPh_3 . After 6 days the intensity of the $^{31}\text{P}\{^1\text{H}\}$ -NMR signal for **16** was dramatically increased, and it was the major component in the reaction mixture. X-ray quality crystals of **16** were obtained as the toluene solvate (see X-ray crystallography section below). Complex **16** was found to be readily soluble in C_7D_8 , which allowed for characterization by $^{29}\text{Si}\{^1\text{H}\}$ and $^{195}\text{Pt}\{^1\text{H}\}$ NMR spectroscopy. The silicon resonance appeared at 239 ppm as a single line flanked by Pt satellites, in a region that is similar to the related triplatinum complexes $[(\text{Ph}_3\text{P})\text{Pt}(\mu\text{-SiC}_{12}\text{H}_8)]_3$ ^{4b} and $[(\text{Me}_3\text{P})\text{Pt}(\mu\text{-Si}(\text{C}_6\text{H}_5)_2)_2]_3$.¹⁹ The $^{195}\text{Pt}\{^1\text{H}\}$ NMR spectrum exhibited a resonance centered at -4352 ppm as a complex pattern due to the presence of ^{195}Pt isotopomers (Figure 1).²¹

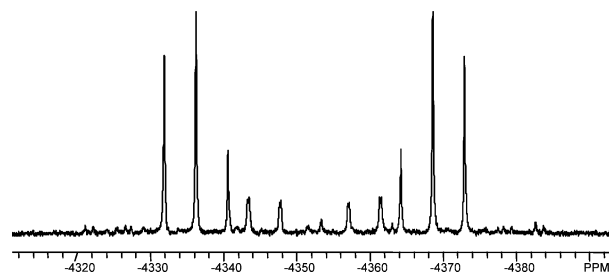
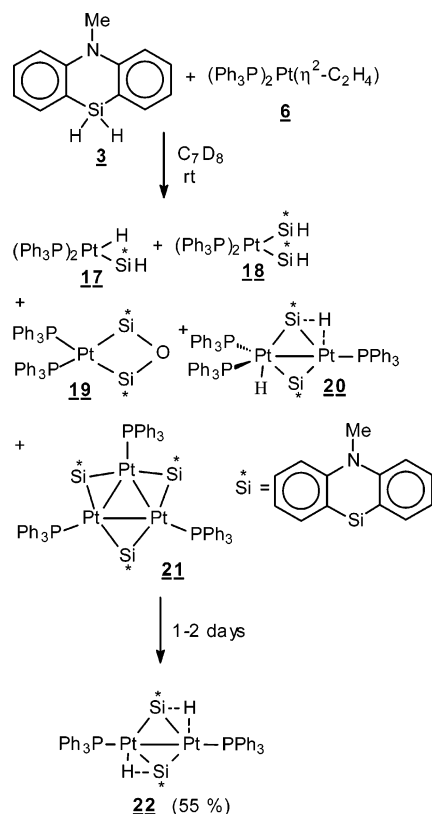


Figure 1. $^{195}\text{Pt}\{^1\text{H}\}$ NMR spectrum (107 MHz, C_7D_8 , 300 K) for complex **16**.

The low-temperature addition reaction of the phenoxasilin precursor **2** to **6** showed results similar to the reaction between **1** and **6** at low temperature. The major resonances observed in the ^1H and $^{31}\text{P}\{^1\text{H}\}$ NMR spectra were for the mononuclear complex **12** and unreacted **6**. As the temperature was warmed

(21) Moor, A.; Pregosin, P. S.; Venanzi, L. M. *Inorg. Chim. Acta* **1981**, *48*, 153.

Scheme 4

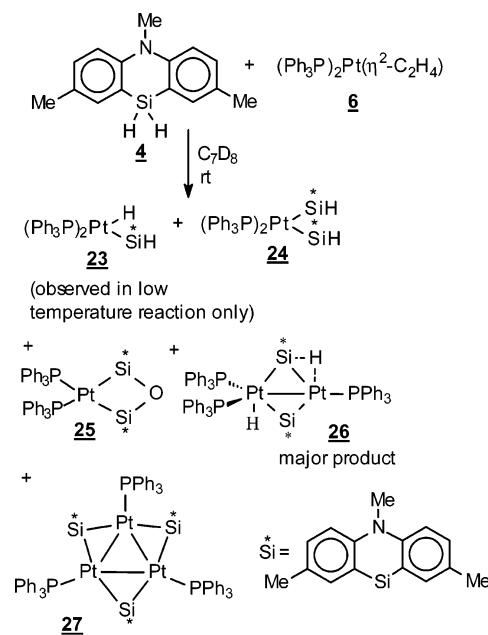


slowly to room temperature in 20 K increments, the signals associated with **6** and **12** began to broaden significantly. At 283 K, the $^{31}\text{P}\{^1\text{H}\}$ NMR spectrum showed a broad peak centered at 25 ppm as the major resonance. When the temperature had reached 303 K, a small-intensity signal was observed for the trinuclear complex **16** in addition to the broad peak at 25 ppm.

Reaction of 5-Methyl-10,10-dihydrophenazasiline (3) with $(\text{Ph}_3\text{P})_2\text{Pt}(\eta^2\text{-C}_2\text{H}_4)$ (6). The room-temperature reaction of **3** with **6** resulted in gas evolution along with the formation of several Pt–Si-containing products, as determined by ^1H and $^{31}\text{P}\{^1\text{H}\}$ NMR spectroscopy. NMR signals for the expected mononuclear complex **17** were observed only in the early stages of the reaction. Minor amounts of the bis(silyl) complex **18**, siloxane complex **19**, and the trinuclear complex **21** were detected by ^{31}P NMR spectroscopy. The major component in the reaction mixture was the unsymmetrical dinuclear complex **20** (Scheme 4). However, after 1–2 days, the symmetrical dinuclear complex **22** was isolated as yellow crystals (55% yield), which were suitable for X-ray crystallography (see X-ray crystallography section below). Signals for **22** were not observed in the reaction mixture by ^1H and $^{31}\text{P}\{^1\text{H}\}$ NMR spectroscopy. It is probable that elimination of a phosphine from **20** occurred to produce complex **22**, which precipitated due to its low solubility in toluene- d_8 . Complex **22** was soluble in CD_2Cl_2 and was characterized by ^1H and $^{31}\text{P}\{^1\text{H}\}$ NMR spectroscopy, X-ray, IR, and elemental analysis. The $^{31}\text{P}\{^1\text{H}\}$ NMR spectrum for **22** exhibited a singlet at 36.9 ppm with two sets of Pt satellites with a pattern similar to that observed for complex **8**.

The low-temperature addition of **3** to **6** resulted in the formation of **17** as the major Pt–Si-containing product. As the temperature was raised from 223 K to room temperature, the NMR signals for **17** started to broaden. After 24 h, complex **22** again precipitated in the NMR tube as the major product. A minor amount of complexes **19** and **21** was also observed in the reaction solution.

Scheme 5



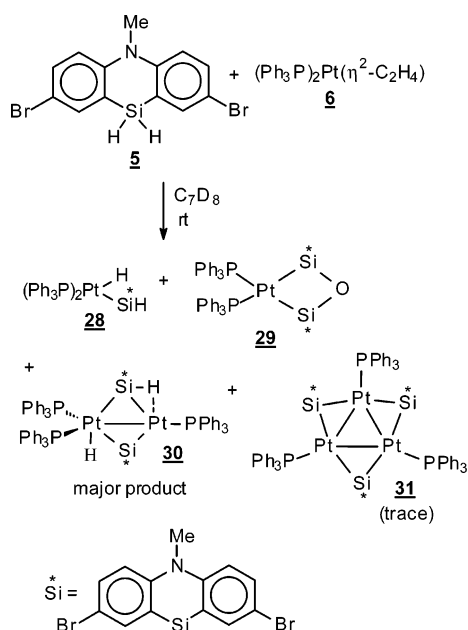
In contrast, when the addition of **3** to **6** was performed at room temperature then immediately placed in a preheated NMR probe at 323 K, NMR signals for the trinuclear complex **21** were observed within 5 min by $^{31}\text{P}\{^1\text{H}\}$ NMR spectroscopy. The low-temperature $^{31}\text{P}\{^1\text{H}\}$ NMR spectra collected 2–3 h after heating to 323 K also indicated the formation of the unsymmetrical dinuclear complex **20**, as well as $\text{Pt}(\text{PPh}_3)_4$ ²⁰ and PPh_3 as the other major reaction components in addition to complex **21**.

Reaction of 2,5,8-Trimethyl-10,10-dihydrophenazasiline (4) with $(\text{Ph}_3\text{P})_2\text{Pt}(\eta^2\text{-C}_2\text{H}_4)$ (6). The room-temperature reaction of **4** with **6** gave results similar to those shown in Scheme 3. The mononuclear complex **23** was observed only when the reaction was performed at low temperature (see below). A broad resonance was observed in the $^{31}\text{P}\{^1\text{H}\}$ NMR spectrum, indicating the formation of the fluxional unsymmetrical dinuclear complex **26** (major product) along with minor sharp signals for the bis(silyl) complex **24**, siloxyplatinum complex **25**, and trinuclear complex **27** (Scheme 5). Upon cooling the solution to 223 K after 1.5 h, well-resolved signals for **26** were observed in the ^1H and $^{31}\text{P}\{^1\text{H}\}$ NMR spectra.

The low-temperature addition of **4** to **6** resulted in the clean formation of complex **23** as the major Pt–Si-containing product along with some unreacted precursor **6**. When the solution was warmed, the signals for **23** began to broaden (263 K), and at room temperature only a broad, ill-defined spectrum was observed (range 0–60 ppm). Upon cooling the solution to 223 K after 5 h, sharp signals for the unsymmetrical dinuclear complex **26** (major species) and unreacted **6** were observed along with minor signals for **25** and **27**.

Reaction of 2,8-Dibromo-5-methyl-10,10-dihydrophenazasiline (5) with $(\text{Ph}_3\text{P})_2\text{Pt}(\eta^2\text{-C}_2\text{H}_4)$ (6). The presence of methyl substituents at the 2,8-positions on the aromatic rings of the heterocyclic hydrosilane precursors as described above does alter the product distribution. However, a much more dramatic effect is observed when bromine substituents are incorporated on the carbon centers *para* to the nitrogen of the heterocycle. The room-temperature reaction of **5** with **6** produced the mononuclear complex **28** initially, but the signals were broad (0–50 ppm in the ^{31}P NMR spectrum). Upon cooling to 223 K after 1 h, sharp resonances were observed for

Scheme 6



the unsymmetrical dinuclear complex **30**. As with the other reactions described herein, a minor amount of the siloxy complex **29** was probably formed, but the ^{31}P NMR signals would overlap with those for **30**. A trace amount of the trinuclear complex **31** was also observed. After 24 h, orange crystalline complex **30** was isolated in 51% yield (Scheme 6).

The low-temperature reaction between **5** and **6** showed results similar to those described above for the other silicon heterocycles. The mononuclear complex **28** was formed as the major product at low temperature, and after reaching room temperature the unsymmetrical complex **30** along with a minor amount of **29** and **31** were present. No signals were observed in either the room-temperature or the low-temperature reaction for a bis(silyl) product, $(\text{Ph}_3\text{P})_2\text{Pt}(\text{SiAr}_2\text{H})_2$.

Discussion

The room-temperature reactions described in the results section above (Schemes 2–6) for the hydrosilanes **1**–**5** with the Pt(0) complex **6** showed that the expected, initially formed mononuclear complexes $(\text{Ph}_3\text{P})_2\text{Pt}(\text{H})(\text{SiAr}_2\text{H})$ (see Table 1) were either highly reactive or thermally unstable. In some reactions minor amounts of mononuclear bis(silyl) complexes $(\text{Ph}_3\text{P})_2\text{Pt}(\text{SiAr}_2\text{H})_2$ were also detected in the early stages of the reaction. The tentative assignments for complexes **9** and **18** are based on spectroscopic data obtained for a related complex that was isolated and characterized for the unsubstituted silafluorene.^{4a} The stable products isolated from these reactions are dinuclear and/or trinuclear complexes.

It is interesting to note that the unsubstituted ring systems **1** and **3** favor the formation of the symmetrical dinuclear complexes $[(\text{Ph}_3\text{P})\text{Pt}(\mu\text{-}\eta^2\text{-HSiAr}_2)]_2$, **8** and **22**. The dinuclear complex **8** is formed within 30 min after addition, but complex **22** precipitated from the reaction solution after 1 to 2 days. Previous results from our laboratory have shown that complexes of this type generally have low solubility in C_6D_6 or C_7D_8 solutions.²² Once the symmetrical dinuclear complex was precipitated in the reaction mixture, further reaction ceased. One notable difference between the reaction of **1** (phenoxasilin) and

6 compared to that between **3** (phenazasilin) and **6** is the absence of any signals for the unsymmetrical dinuclear complex $(\text{Ph}_3\text{P})_2(\text{H})\text{Pt}(\mu\text{-SiAr}_2)(\mu\text{-}\eta^2\text{-HSiAr}_2)\text{Pt}(\text{PPh}_3)$ in the former reaction. In contrast, the major product initially formed in the reaction between **3** and **6** was the unsymmetrical dinuclear complex **20**. Our previous results suggested that the fluxional process observed for related unsymmetrical dinuclear complexes probably involved dissociation/coordination of a phosphine at the dinuclear framework proceeding through a symmetrical dinuclear intermediate such as **8** and **22**.^{4a}

The formation of trinuclear complexes $[(\text{Ph}_3\text{P})\text{Pt}(\mu\text{-SiAr}_2)]_3$, **11** and **21**, from the reaction of **1** and **6** or between **3** and **6**, respectively, at room temperature did not occur at all or only to a minor extent (**3** + **6**). However, the magnitude of trimer formation could be increased when the addition was performed followed by immediate heating of the reaction solution to 323 K. The mechanism of formation of the trinuclear complex is not known but may involve a bimolecular reaction between two dinuclear species or between a mononuclear and dinuclear species.

We previously found that incorporation of substituents on the aromatic ring had a significant effect on the reactivity of **6** with silafluorene compared to 3,7-di-*tert*-butylsilafluorene with precursor **6**.⁴ In the former reaction, mononuclear (not isolated), unsymmetrical dinuclear and trinuclear complexes were observed by NMR spectroscopy. However, the substituted silafluorene provided the unsymmetrical dinuclear complex $(\text{Ph}_3\text{P})_2(\text{H})\text{Pt}(\mu\text{-SiC}_{20}\text{H}_{24})(\mu\text{-}\eta^2\text{-HSiC}_{20}\text{H}_{24})\text{Pt}(\text{PPh}_3)$ as the major product in 86% yield.^{4b} The presence of the bulky *tert*-butyl groups at the ring positions *meta* to the silicon center inhibited the formation of the trinuclear complex. We anticipated that placement of other groups such as methyl would have a similar effect. Surprisingly, reaction of 2,8-dimethylphenoxasilin **2** with **6** produced not only the expected mononuclear complex **12** from Si-H bond activation and the unsymmetrical dinuclear complex **15** but also the trinuclear complex **16** was eventually isolated in nearly quantitative yield. The reaction of silane precursor **4** with **6** provided similar results, but significant amounts of both dinuclear **26** and trinuclear complex **27** were formed. The 2,8-dibromophenoxasilin precursor **5** produced very little trinuclear complex **31** upon reaction with complex **6**, and the unsymmetrical complex **30** was the major product formed. The presence of the electronegative Br substituents appears to inhibit the formation of the trinuclear complex.

Multinuclear NMR spectroscopy is a powerful tool to determine the types of products formed in the reactions shown in Schemes 2–6. Similar chemical shifts, multiplicity patterns, and coupling constant values are observed for complexes of the same general structural type as shown in Table 1. For example, mononuclear complexes of the type $(\text{Ph}_3\text{P})_2\text{Pt}(\text{H})(\text{SiAr}_2\text{H})$ (**7**, **12**, **17**, **23**, **28**) show two distinct hydride resonances in the ^1H NMR spectrum, near 5 ppm (multiplet, SiH) and -1.5 ppm (doublet of doublets with prominent Pt satellites, PtH). The two phosphines are inequivalent and therefore couple to each other, giving rise to two doublets (near 30–35 ppm) each with one set of Pt satellites in the ^{31}P NMR spectrum. The strong *trans* influence exerted by silicon results in a smaller $^1J_{\text{PtP}}$ coupling (~ 1800 Hz) for the phosphorus center positioned *trans* to silicon compared to ~ 2400 Hz for the phosphine *cis* to silicon.²³ A number of stable mononuclear complexes $(\text{R}'_3\text{P})_2\text{Pt}(\text{H})(\text{SiR}'_2\text{R}'')$ are known.²⁴

The unsymmetrical dinuclear complexes $[(\text{Ph}_3\text{P})_2(\text{H})\text{Pt}(\mu\text{-SiR}_2)(\mu\text{-}\eta^2\text{-HSiR}_2)\text{Pt}(\text{PPh}_3)]$ (**15**, **20**, **26**, and **30**) are unusual since they have two distinct sites each for Pt, P, Si, and H. The

(22) Braddock-Wilking, J.; Levchinsky, Y.; Rath, N. P. *Organometallics* **2000**, *19*, 5500.

bridging hydride participates in a nonclassical, 3c-2e interaction with Pt and Si ($\text{Pt}\cdots\text{H}\cdots\text{Si}$).^{1,2c,f,i} The ^1H NMR spectra for the unsymmetrical dinuclear complexes (Table 1) show two unique resonances for complexes **15** and **30**; however, the bridging hydrides were not located for **20** and **26** and were probably obscured by other resonances. For complexes **15** and **30** a signal appears near 3 ppm as a doublet as a consequence of coupling to one phosphine for the ($\text{Pt}\cdots\text{H}\cdots\text{Si}$) unit; however, the J_{SiH} and J_{PtH} coupling values could not be resolved. The other unique resonance appears at a lower frequency between -5 and -6 ppm generally as a triplet with two sets of Pt satellites for the terminal Pt-H.⁴

The ^{31}P NMR spectra at room temperature for the unsymmetrical dinuclear complexes exhibit a broadened signal centered near 10–20 ppm, indicating fluxional behavior on the NMR time scale. Related unsymmetrical dinuclear Pt complexes containing bridging silafluorenyl groups^{4a} and Pd complexes with ($\mu\text{-SiPh}_2$)²⁵ units were also reported to exhibit dynamic temperature-dependent NMR spectra, by a proposed mechanism involving dissociation of one of the two equivalent phosphines followed by recoordination of the phosphine at the other metal center. In the former case, the mechanism could also involve concomitant transformation of bridging and terminal hydrides.^{4a} Exchange of free (*p*-Tol)₃P with coordinated Ph₃P was recently confirmed for an unsymmetrical dinuclear Pt₂ complex containing silafluorenyl bridging ligands.^{4a} However, the low-temperature (-50 °C) spectra for the unsymmetrical dinuclear complexes show resolved resonances for the two different phosphorus environments. The two equivalent phosphines, (Ph_3P)₂Pt, couple to the other phosphine Pt(PPh_3) and afford a doublet (near 20 ppm) and a triplet (near 30 ppm) pattern, respectively, each with two sets of Pt satellites due to the presence of two Pt centers in the complex.⁴ Similar ^1H and ^{31}P NMR spectral features were observed for a mixed Pt–Pd unsymmetrical dinuclear complex reported by Osakada et al.²⁶

In contrast, the symmetrical dinuclear complexes [$(\text{Ph}_3\text{P})\text{-Pt}(\mu\text{-}\eta^2\text{-HSiR}_2)_2$] (**8** and **22**) display one type of hydride ($\text{Pt}\cdots\text{H}\cdots\text{Si}$) in the ^1H NMR spectrum generally near 1–3 ppm, in the region often observed for other related symmetrical dinuclear Pt–Pt and Pd–Pd and mixed Pt–Pd complexes containing ($\mu\text{-}\eta^2\text{-HSiR}_2$) units.^{4a,16,17,22,25–27} Recently, the NMR chemical shifts were predicted for the related hypothetical complex [$\text{Pd}_2(\text{SiH}_3)_2(\text{PH}_3)_2$]. The hydride shift in the ^1H NMR spectrum was calculated to be 2.11 ppm and can be described as a hydride that lies between a silyl hydride and a metal hydride environment.²⁸ The symmetrical environment in these complexes gives rise to one type of phosphorus environment, leading to a sharp ^{31}P resonance with two sets of Pt satellites as part of an AA'XX' spin system with large $^1J_{\text{PtP}}$ coupling values.^{4a,16,17,26} The symmetrical dinuclear complexes described in the current work did not show fluxional NMR behavior.

(23) (a) Appleton, T. G.; Clark, H. C.; Manzer, L. E. *Coord. Chem. Rev.* **1973**, *10*, 335. (b) Coe, B. J.; Glenwright, S. J. *Coord. Chem. Rev.* **2000**, *203*, 5.

(24) See for example: Chan, D.; Duckett, S. B.; Heath, S. L.; Khazal, I. G.; Perutz, R. N.; Sabo-Etienne, S.; Timmins, P. L. *Organometallics* **2004**, *24*, 5744.

(25) (a) Kim, Y.-J.; Lee, S.-C.; Park, J.-I.; Osakada, K.; Choi, J.-C.; Yamamoto, T. *Organometallics* **1998**, *17*, 4929. (b) Kim, Y.-J.; Lee, S.-C.; Park, J.-I.; Osakada, K.; Choi, J.-C.; Yamamoto, T. *J. Chem. Soc., Dalton Trans.* **2000**, 417.

(26) Yamada, T.; Tanabe, M.; Osakada, K.; Kim, Y.-J. *Organometallics* **2004**, *23*, 4771.

(27) Sanow, L. M.; Chai, M.; McConnville, D. B.; Galat, K. J.; Simons, R. S.; Rinaldi, P. L.; Youngs, W. J.; Tessier, C. A. *Organometallics* **2000**, *19*, 192.

(28) Nakajima, S.; Sumimoto, M.; Nakao, Y.; Sato, H.; Sakaki, S.; Osakada, K. *Organometallics* **2005**, *24*, 4029.

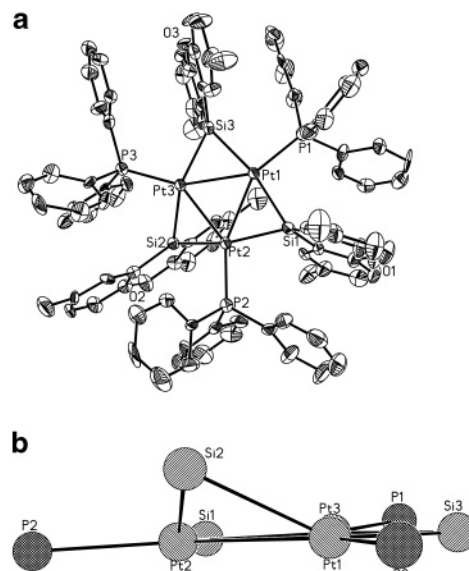


Figure 2. (a) Molecular structure of **16** (as 2.5 C_7D_8 solvate). Selected bond lengths (Å) and angles (deg): Pt1–Pt2 2.7386(6), Pt1–Pt3 2.7138(6), Pt2–Pt3 2.7199(7), Pt1–P1 2.252(3), Pt2–P2 2.247(3), Pt3–P3 2.2469(3), Pt1–Si1 2.379(3), Pt1–Si3 2.373(3), Pt2–Si1 2.336(3), Pt2–Si2 2.360(3), Pt3–Si2 2.356(3), Pt3–Si3 2.332(3); Pt2–Pt1–Pt3 59.843(16), Pt1–Pt2–Pt3 59.625(16), Pt2–Pt3–Pt1 60.532(16), Pt1–Si1–Pt2 71.01(9), Pt2–Si2–Pt3 70.45(8), Pt3–Si(3)–Pt1 70.43(9). (b) Core structure of **16**.

The trinuclear complexes [$(\text{Ph}_3\text{P})\text{Pt}(\mu\text{-SiR}_2)_3$] (**11**, **16**, **21**, **27**, and **31**) contain only aromatic or methyl resonances and no Pt–H or ($\text{Pt}\cdots\text{H}\cdots\text{Si}$) signals in the ^1H NMR spectrum. The $^{31}\text{P}\{^1\text{H}\}$ NMR spectrum for the trinuclear complexes shows a resonance near 70 ppm with a complex Pt satellite pattern due to the presence of several isotopomers containing ^{195}Pt .²¹ The presence of ^{195}Pt -containing isotopomers also results in a complex ^{195}Pt NMR spectrum (see Figure 1).²¹ The ^{29}Si NMR signals for the trinuclear complexes **16** and **21** were observed at high frequency, near 240–250 ppm, in a region often observed for bridging ($\mu\text{-SiR}_2$) groups.^{2f}

The structures of complexes **16**, **22**, and **30** were confirmed by X-ray crystallography. The molecular structures of the deep red trinuclear complex **16** along with selected bond distances and angles are shown in Figure 2.

Complex **16** exhibits a nonplanar Pt_3Si_3 core. One of the silicon centers (Si2) in one of the phenoxasilin ring systems lies above the plane defined by the remaining Pt_3Si_2 atoms by ca. 1.1 Å, and the phosphorus (P1) center lying opposite (Si2) also lies above that plane by ca. 0.2 Å. This solid state arrangement is likely due to packing forces. A similar solid state environment was also observed for the trinuclear complex [$(\text{Ph}_3\text{P})\text{Pt}(\mu\text{-SiC}_{12}\text{H}_8)_3$]^{4b,c} and the related complex (Me_3P)Pt($\mu\text{-SiPh}_2$)₃,¹⁹ both of which exhibited a nonplanar Pt_3Si_3 core. The Pt–Pt, Pt–P, and Pt–Si bond distances found in **16** are within the expected range.¹

Complex **22** was isolated as an off-white crystalline solid, and the molecular structure is shown in Figure 3 along with selected bond distances and angles. Complex **22** exhibits a planar central $\text{P}_2\text{Pt}_2\text{Si}_2$ core due to a center of inversion. The hydrides were located but not refined and were found to lie above and below the central core, in contrast to related symmetrical dinuclear complexes, where the bridging hydrides are found in the same plane as the $\text{P}_2\text{Pt}_2\text{Si}_2$ atoms.

The presence of the nonclassical ($\text{Pt}\cdots\text{H}\cdots\text{Si}$) interaction in **22** is supported by the solution NMR and IR spectroscopic data

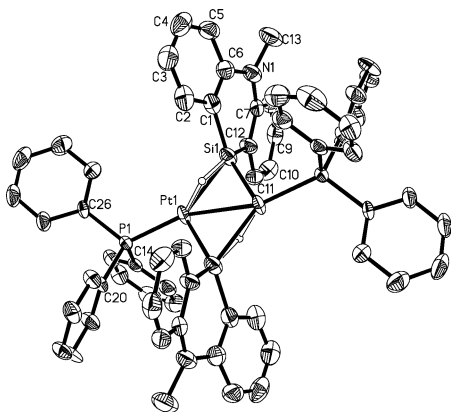


Figure 3. Molecular structure of **22** (as C_7D_8 solvate). Selected bond lengths (\AA) and angles (deg): Pt1–Pt#1 2.7032(6), Pt1–P1 2.254(2), Pt1–Si1 2.411(2), Pt1–Si3 2.322(3), Pt1–H11a 1.54, Si1–H11a 1.64; P1–Pt1–Pt#1 161.81(6), Pt1–Si1–Pt#1 69.63(7), Si1–Pt1–Si#1 110.37(7), P1–Pt1–Si#1 105.21(8), P1–Pt1–Si1 144.34(9).

as well as the X-ray crystal structure. Two different and alternating Pt–Si distances, 2.32 and 2.41 \AA , are found in the solid state structure for **22**, where the longer distance is associated with the Pt–Si bond bridged by the hydride. Another notable feature found in the structure of **22** is the nonlinear P1–Pt1–Pt#1 angle (162°). Related symmetrical dinuclear complexes also exhibit the same phenomenon where the phosphine bends away from the position of the bridging hydride.^{16,17,22,25,26} In complexes where the $(\text{Pt}\cdots\text{H}\cdots\text{Si})$ hydrides have been located and refined by X-ray crystallography, elongated Pt–H and Si–H distances are often observed, supporting the nonclassical 3c–2e interaction.^{1,2c,i} Although these distances involve unrefined H-positions (for **22** and **30**) where the distances are not as accurate as those between heavier elements, a general bonding environment can be deduced from the structure.

A recent theoretical study examined the bonding nature in silyl-bridged dinuclear $\text{M}_2(\text{SiH}_3)_2(\text{PH}_3)_2$ ($\text{M} = \text{Pd}, \text{Pt}$) complexes.²⁸ The bonding environment in the complexes was described as not a pure silyl group but having some silylene ($\mu\text{-SiR}_2$) and hydride type character and can be represented by the formula $\text{M}_2(\mu\text{-}\eta^2\text{-H}\cdots\text{SiH}_2)_2(\text{PH}_3)_2$. The Pt–Pt bond was considered to be stronger than a Pd–Pd bond in the complexes $\text{M}_2(\text{SiH}_3)_2(\text{PH}_3)_2$, and the nonclassical interaction between the Si–H bond and Pt was stronger than in the Pd system. The calculated bond distances for $\text{Pt}_2(\text{SiH}_3)_2(\text{PH}_3)_2$ were in good agreement with our experimental results (Pt–Pt 2.742 \AA ; Pt–P 2.281 \AA ; Pt–Si 2.372 \AA , 2.480; Pt \cdots H 1.775 \AA ; Si \cdots H 1.715 \AA).²⁸ Other recent theoretical calculations for complexes with the formula $[\text{L}_n\text{M}(\mu\text{-}\eta^2\text{-HSiR}_2)]_2$ were found to exhibit shorter Si \cdots H distances compared to mononuclear $[\text{L}_n\text{M}(\eta^2\text{-HSiR}_3)]$ complexes due to the weaker back-donation from the metal to the Si–H(σ^*) orbital.²⁹

The orange, unsymmetrical dinuclear complex **30** was also structurally characterized by X-ray crystallography. The molecular structure of **30** is shown in Figure 4 along with selected bond distances and angles. The general structural features of **30** are similar to those found for the related unsymmetrical dinuclear complex $[(\text{Ph}_3\text{P})_2(\text{H})\text{Pt}(\mu\text{-SiC}_{20}\text{H}_{24})\text{-}(\mu\text{-}\eta^2\text{-HSiC}_{20}\text{H}_{24})\text{Pt}(\text{PPh}_3)]$,^{4b} dipalladium complex $(\text{Me}_3\text{P})\text{Pd}(\mu\text{-HSiPh}_2)_2\text{Pd}(\text{PMe}_3)_2$,^{25a} and mixed Pt–Pd complex $(\text{Et}_3\text{P})_2\text{-Pt}(\mu\text{-}\eta^2\text{-HSiPh}_2)\text{Pd}(\text{PEt}_3)$.²⁶ Complex **30** exhibits an unsymmetrical

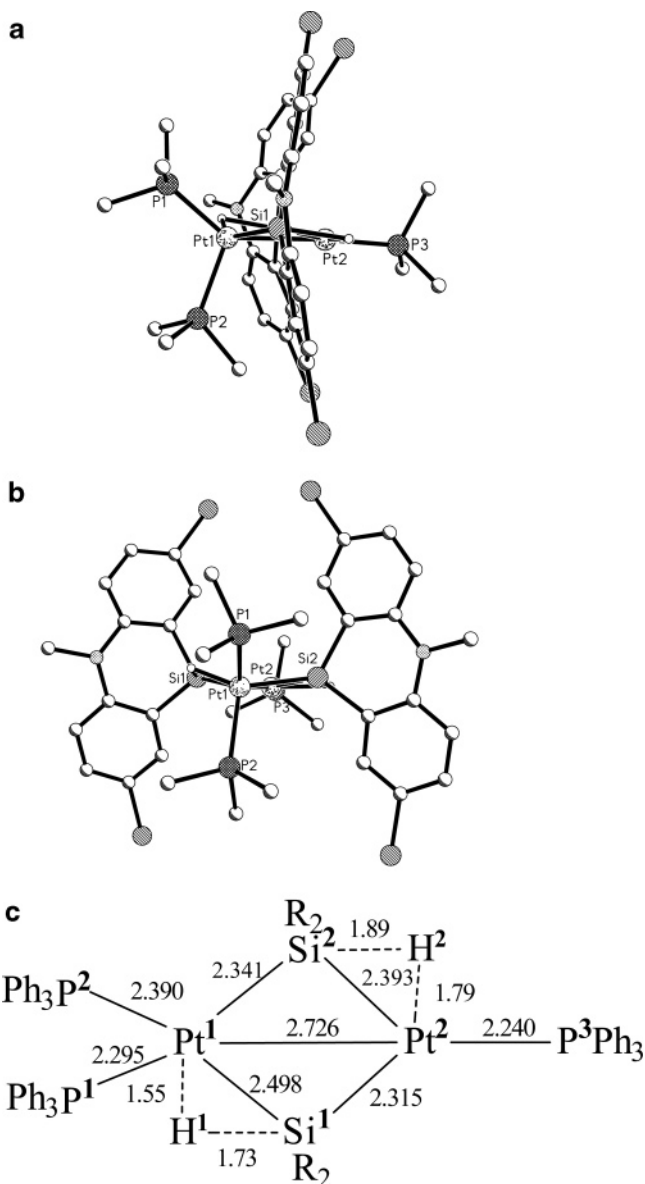


Figure 4. (a) Molecular structure of **30** (as 3 C_7D_8 solvate). Selected bond lengths (\AA) and angles (deg): Pt1–Pt2 2.7268(2), Pt1–P1 2.2952(12), Pt1–P2 2.3902(12), Pt2–P3 2.24029(12), Pt1–Si1 2.4984(13), Pt1–Si2 2.3409(13), Pt2–Si1 2.3151(13), Pt2–Si2 2.3931(13), Pt1–H1 1.55, Si1–H1 1.73, Pt2–H2 1.79, Si2–H2 1.89; P1–Pt1–P2 110.41(4), P3–Pt2–Pt1 163.56(3), Si1–Pt1–Si2 106.46(4), Si1–Pt2–Si2 110.88(4), Pt1–Si1–Pt2 68.89(4), Pt1–Si2–Pt2 70.33(4), P2–Pt1–Pt2 108.93(3), P1–Pt1–Pt2 137.34(3). (b) Molecular structure of **30** viewed along the Pt–Pt bond. (c) Core structure of **30** showing selected bond distances.

environment in the solid state. Four distinct Pt–Si distances were found (Figure 4). The longest distances (ca. 2.4–2.5 \AA) were observed between Pt1–Si1 and Pt2–Si2. The two hydrides in **30** were located but not refined. The hydride bound to Pt1–H1 showed a shorter distance (1.55 \AA) to the metal center than the distance to the silicon center (Si1–H1, 1.73 \AA), in agreement with the low-temperature solution state assignment of H1 as terminal hydride. However, the Si–H distance is within the range observed for nonclassical $(\text{Pt}\cdots\text{H}\cdots\text{Si})$ interactions, suggesting that some interaction is possible in the solid state.^{1,2c,i} Much longer distances were found with the other hydride (Pt2–H2, ca. 1.8 \AA and Si2–H2, ca. 1.9 \AA), in agreement with the low-temperature NMR assignment for a bridging environment

(29) (a) Choi, S.-H.; Lin, Z. *J. Organomet. Chem.* **2000**, 608, 42. (b) Lin, Z. *Chem. Soc. Rev.* **2002**, 31, 239.

for this hydride. The dihedral angle between the hydrides H1–Pt1–Pt2–H2 was found to be 158°.

The reactivity of several silicon-containing tricyclic ring systems **1–5** with the Pt(0) phosphine complex **6** was examined and a variety of different products were obtained depending upon the silicon precursor used. In all cases, mononuclear complexes of the type P₂Pt(H)(SiR₂H) (or P₂Pt(SiR₂H)₂) were believed to be the initial products formed at room temperature but were found to be highly reactive (or thermally unstable). Dinuclear or trinuclear complexes were isolated as the major products from these reactions. The unsubstituted ring systems **1** and **3** provided symmetrical dinuclear complexes [(Ph₃P)Pt(μ-η²-HSiR₂)₂] (**8** and **22**). In contrast, the methyl-substituted ring system **2** provided the trinuclear complex [(Ph₃P)Pt(μ-SiR₂)₃] (**16**) in almost quantitative yield, and precursor **4** also provided significant amounts of the trinuclear complex **27** along with the unsymmetrical dinuclear complex [(Ph₃P)₂(H)Pt(μ-SiR₂)(μ-η²-HSiR₂)Pt(PPh₃)] (**26**). The bromo-substituted silane **5** provided the unsymmetrical complex **30** in high yield. The structures of complexes **16**, **22**, and **30** were confirmed by X-ray crystallography. Current studies are underway to examine the reactivity and potential catalytic activity of these di- and trinuclear complexes.

Experimental Section

General Procedures. All glassware was oven- or flame-dried prior to use. Reactions were performed (or samples prepared) under an argon or nitrogen atmosphere either on a double-manifold Schlenk line or in an inert atmosphere drybox. Diethyl ether was distilled over Na/benzophenone and THF was distilled over Na/9-fluorenone before use. Silicon tetrachloride (Acros Organics) and trichlorosilane (Aldrich) were distilled over anhydrous K₂CO₃ before use. Diphenyl ether (Fisher Scientific), di-*p*-tolyl ether (TCI America or Aldrich), *N*-methylidiphenylamine (Acros Organics), di-*p*-tolylamine (Aldrich or TCI America), lithium aluminum hydride (or deuteride) powder (Aldrich), *n*-butyllithium (Aldrich), ethylene-(bis)triphenylphosphine platinum(0) (Aldrich), and tetrakis(triphenylphosphine)platinum(0) (Strem) were used as received. TMEDA (Aldrich or Acros Organics) was distilled over KOH before use. 2,8-Dibromo-5-methyl-10,10-dihydrophenazasiline (**5**) was prepared according to a literature procedure.⁵ Toluene-*d*₈, benzene-*d*₆, and methylene chloride-*d*₂ were purchased from Cambridge Isotopes, Inc., and for experiments involving an inert atmosphere the solvents were degassed by freeze–pump–thaw vacuum cycles and stored over activated molecular sieves inside an inert atmosphere drybox.

NMR spectroscopic data were recorded on a Bruker ARX-500 spectrometer at 500 MHz for ¹H, 99 MHz for ²⁹Si, 125 MHz for ¹³C, and 202 MHz for ³¹P. Proton chemical shifts (δ) are reported relative to residual protonated solvent: CDCl₃ (7.27 ppm), C₆D₆ (7.15 ppm), CD₂Cl₂ (5.32 ppm), and C₇D₈ (2.09 ppm). Carbon chemical shifts are reported relative to solvent: CDCl₃ (77.23 ppm) and C₆D₆ (128.39 ppm). Silicon chemical shifts (δ) are reported relative to external TMS (0 ppm). Phosphorus chemical shifts (δ) are reported relative to external H₃PO₄ (0 ppm). Chemical shifts are given in ppm and coupling constants in Hz. NMR data were collected at ambient temperature unless otherwise noted.

The majority of the NMR data listed for reaction mixtures formed from Pt and Si precursors includes selected key resonances that are characteristic for the particular product, and resonances for aromatic protons, for example, are not included since there are many overlapping resonances. Infrared spectra were recorded on a Thermo-Nicolet Avatar 360 E.S.P. FT-IR spectrometer. GC-MS (EI) data were recorded on a Hewlett-Packard GC/MS System Model 5988A, and *m/e* values of ≥10% of the base peak are indicated. The X-ray crystal structure determinations were performed on a Bruker SMART 1K diffractometer equipped with a

CCD area detector at 233 K. Melting points were obtained using a Thomas-Hoover capillary melting point apparatus and are uncorrected. Elemental analysis determinations were performed by Atlantic Microlabs, Inc., Norcross, GA.

Preparation of 10,10-Dihydrophenoxasilin (1). A modified literature procedure was used.^{8,9} A solution of Ph₂O (16.9 g, 99.4 mmol) in 125 mL of anhydrous THF was cooled to –30 °C, and *n*-BuLi (120 mL, 2.5 M in hexanes, 300 mmol) was added dropwise. The solution was warmed to room temperature overnight. The resulting solution was added dropwise to distilled SiCl₄ (26.8 g, 157.9 mmol) in 60 mL of anhydrous THF at –78 °C over 3 h. The solution was warmed to room temperature and stirred overnight. The volatile materials were then removed, and 100 mL of freshly distilled Et₂O was added. **Caution: Failure to remove unreacted SiCl₄ before treatment with LiAlH₄ can result in the formation of pyrophoric silane, SiH₄.** Lithium aluminum hydride (2.6 g, 70 mmol) was added slowly at 0 °C over approximately 3 h. After warming to room temperature overnight, the solution was hydrolyzed with saturated aqueous NH₄Cl. The bright yellow organic layer was extracted and washed with water, then dried over MgSO₄. The product was purified by Kugelrohr distillation at 65–67 °C/0.2 mmHg (3.8 g, ca. 19% yield). Further purification was achieved by preparative gas chromatography. ¹H NMR (500 MHz, CDCl₃): δ 7.58 (dd, 2H, *J* = 7, 2, aromatic ArH), 7.47 (dt, 2H, *J* = 8, 2, ArH), 7.22 (d, 2H, *J* = 8, ArH), 7.16 (t, 2H, *J* = 7, ArH), 4.96 (s, 2H, ¹J_{SiH} = 211 Hz, SiH). ¹³C{¹H} NMR (125 MHz, CDCl₃): δ 160.5, 135.9, 132.2, 122.9, 118.6, 110.7. ²⁹Si{¹H} NMR (99 MHz, DEPT, CDCl₃): δ –63.6. IR (neat) (ν, cm^{–1}): 2139 (SiH). GC-MS (EI, 70 eV): *m/z* (%) 198 (M⁺, 76), 197 (M⁺ – H, 100), 152 (39), 121 (13), 77 (21). HR-MS (EI, 70 eV): calcd for C₁₂H₁₀OSi, 198.05009; found, 198.0501.

Preparation of 2,8-Dimethyl-10,10-dihydrophenoxasilin (2). A reaction sequence similar to that described above was used for the preparation of compound **2** by addition of *n*-BuLi (2.5 M, 30 mL, 75 mmol) to *p*-tolyl ether (4.9 g, 25 mmol) in 35 mL of THF at –78 °C. The resulting solution was then transferred and added to silicon tetrachloride (3.5 mL, 5.2 g, 31 mmol) in diethyl ether (50 mL) at –78 °C. The reduction reaction was performed with LiAlH₄ (0.64 g, 17 mmol). After the usual workup, the organic fraction was purified by Kugelrohr distillation, bp 112–140 °C/0.2 mm, providing a white solid. Recrystallization from hot ethanol gave product **2** (0.61 g, 11%), mp 94–95 °C. ¹H NMR (300 MHz, CDCl₃): δ 7.36 (m, 2H, ArH), 7.25 (dd, 2H, *J* = 8, 2, ArH), 7.09 (d, 2H, *J* = 8, ArH), 4.91 (s, 2H, ¹J_{Si–H} = 210 Hz), 2.36 (s, 6H, ArMe). ¹³C{¹H} NMR (125 MHz, CDCl₃): δ 158.6, 135.7, 133.0, 131.9, 118.3, 110.2, 20.7 (Ar–Me). ²⁹Si{¹H} NMR (99 MHz, DEPT, CDCl₃): δ –63.5. IR (solid) (ν, cm^{–1}): 2159 (SiH). GC-MS (EI, 70 eV): *m/z* (%) 226 (M⁺, 100), 211 (20), 166 (20), 165 (34), 91 (20), 89 (14), 65 (10). Anal. Calcd for C₁₄H₁₄OSi: C, 74.29; H, 6.23. Found: C, 74.22; H, 6.31.

Preparation of 5-Methyl-10,10-dihydrophenazasiline (3). A 250 mL round-bottom flask was charged with *N*-methylidiphenylamine (12 mL, 68 mmol), TMEDA (21 mL, 136 mmol), and hexanes (50 mL). A solution of *n*-BuLi (60 mL, 2.5 M in hexanes, 142 mmol diluted with an additional 34 mL of hexanes) was added to the flask dropwise at room temperature. The resulting orange-yellow reaction mixture was refluxed for 4 h, then cooled to room temperature. The mixture was filtered to remove a soluble fraction,³⁰ and the remaining white insoluble lithium reagent was then dissolved in Et₂O (170 mL). Silicon tetrachloride (10.5 mL, 15.6 g, 91.7 mmol) in Et₂O (4 mL) was added over 15 min at –78 °C. The reaction mixture was warmed to room temperature, and after 24 h, the volatile material was removed. Diethyl ether (120 mL) was added to the reaction flask, and the contents were cooled to 0 °C followed by slow addition of solid LiAlH₄ (1.4 g, 37 mmol). After stirring overnight, the reaction mixture was quenched with

(30) Bennett, B. K.; Richmond, T. G. *J. Chem. Educ.* **1998**, *75*, 1034.

saturated NH_4Cl (25 mL). The organic layer was extracted with Et_2O and dried over MgSO_4 . GC analysis of the crude reaction mixture indicated the desired product comprised 59% of the reaction products. After removal of the volatile material, a Kugelrohr distillation (110–115 °C/0.1 mmHg) was attempted but did not provide adequate separation of **3** from the other impurities. A pure sample of **3** was obtained by recrystallization of the distilled material from hexanes/ CH_2Cl_2 (70/30) and gave 5-methyl-10,10-dihydrophenazasilin (**3**) as a tan solid in 4% isolated yield (0.49 g): mp 95–96 °C. ^1H NMR (500 MHz, CDCl_3): δ 7.60 (d, 2H, $J = 7$, ArH), 7.44 (t, 2H, $J = 8$, ArH), 7.11 (d, 2H, $J = 8$, ArH), 7.06 (t, 2H, $J = 7$, ArH), 4.90 (s, 2H, $^1J_{\text{Si-H}} = 206$, SiH), 3.57 (s, 3H, NCH_3). $^{13}\text{C}\{^1\text{H}\}$ NMR (125 MHz, CDCl_3): δ 151.9, 135.5, 130.9, 120.9, 115.6, 115.5, 38.4 (NMe). $^{29}\text{Si}\{^1\text{H}\}$ NMR (99 MHz, DEPT, CDCl_3): δ -55.0. IR (solid) (ν , cm^{-1}): 2097 (Si-H). GC-MS (EI, 70 eV) m/z (%): 211 (100, M^+), 210 (57), 196 (19), 182 (14), 181 (79, $\text{M} - \text{SiH}_2$), 180 (36), 105 (12). Anal. Calcd for $\text{C}_{13}\text{H}_{13}\text{NSi}$: C, 73.88; H, 6.20. Found: C, 73.79; H, 6.11.

Synthesis of 2,5,8-Trimethyl-10,10-dihydrophenazasilin (4 and 4-d₂). Butyllithium (7.1 mL, 15 mmol) was added dropwise to a flask containing a solution of *N*-methyl-*o,o'*-dibromodi-*p*-tolylamine (2.8 g, 7.6 mmol)³¹ in Et_2O (50 mL) at -78 °C. After ca. 30 min the temperature was raised slowly to 0 °C, then the mixture was stirred for approximately 1 h. The resulting reaction mixture was added dropwise to a solution of HSiCl_3 (1.2 mL, 12 mmol) in Et_2O (35 mL). After stirring for 19 h at room temperature, the reaction mixture was treated slowly with lithium aluminum hydride (0.7 g, 18.4 mmol). **Caution: Failure to remove unreacted HSiCl_3 before treatment with LiAlH_4 can result in the formation of pyrophoric silane, SiH_4 .** After 48 h more Et_2O was added (100 mL) followed by the slow addition of saturated ammonium chloride (15 mL). The organic layer was extracted and the aqueous layer washed with Et_2O (80 mL). The combined organic layers were dried over anhydrous MgSO_4 . The organic residue was filtered and the solvent removed under reduced pressure. The crude product was recrystallized from hot EtOH , and the desired product (**4**) was isolated in 42% yield (0.78 g, mp 103.0–104.5 °C). A similar procedure that utilized silicon tetrachloride instead of trichlorosilane was also attempted, but significantly lower yields of **4** were obtained during efforts to remove impurities in the sample.

An analogous reaction was also performed to produce the deuterium analogue 2,5,8-trimethyl-10,10-dideuterophenazasilin (**4-d₂**) starting from *N*-methyl-*o,o'*-dibromodi-*p*-tolylamine (2.0 g, 5.4 mmol), *n*-BuLi (5.4 mL, 13.5 mmol), SiCl_4 (1 mL, 8 mmol), and LiAlD_4 (0.43 g, 10.2 mmol). After workup, the product was isolated in 24% yield (0.31 g), mp 102–104 °C.

Characterization Data for 4. ^1H NMR (300 MHz, C_6D_6): δ 7.33 (d, 2H, $J = 2$, ArH), 7.06 (dd, 2H, $J = 8$, 2, ArH), 6.71 (d, 2H, $J = 8$, ArH), 5.15 (s, 2H, $^1J_{\text{SiH}} = 204$, SiH), 2.97 (s, 3H, NCH_3), 2.16 (s, 6H, ArCH_3). $^{13}\text{C}\{^1\text{H}\}$ NMR (75 MHz, C_6D_6): δ 150.6, 136.5, 131.9, 129.8, 115.9, 115.7, 38.2 (NCH_3), 20.8 (ArCH_3). $^{29}\text{Si}\{^1\text{H}\}$ NMR (99 MHz, DEPT, C_6D_6): δ -55.2. IR (solid) (ν , cm^{-1}): 2113 (SiH). GC-MS (EI, 70 eV): m/z (%) 239 (M^+ , 100), 238 (42), 224 (24), 209 (78), 194 (11), 119 (10).

Characterization Data for 4-d₂. ^1H NMR (300 MHz, CDCl_3): δ 7.40 (d, 2H, $J = 2$, ArH); 7.23 (dd, 2H, $J = 8$, 2, ArH), 6.99 (d, 2H, $J = 8$, ArH), 3.51 (s, 3H, NCH_3), 2.34 (s, 6H, ArCH_3). ^2H NMR (76 MHz, $\text{CHCl}_3/\text{CDCl}_3$): δ 4.92 (s, SiD, $^1J_{\text{SiD}} = 32$). $^{29}\text{Si}\{^1\text{H}\}$ NMR (99 MHz, DEPT, C_6D_6): δ -55.6 (pent, $^1J_{\text{SiD}} = 31$). IR (solid) (ν , cm^{-1}): 1551 (SiD). Anal. Calcd for $\text{C}_{15}\text{H}_{15}\text{D}_2\text{NSi}$: C, 74.63; H, 7.93. Found: C, 74.42; H, 7.24.

General Procedure for Low-Temperature Addition Reactions. The reactions are typically run in a 1:1 ratio between the

platinum and hydrosilane precursors. A solution of the platinum precursor $(\text{Ph}_3\text{P})_2\text{Pt}(\eta^2\text{-C}_2\text{H}_4)$ (**6**) was made in approximately 0.5–0.75 mL of C_7D_8 and transferred to a NMR tube capped with a rubber septum. In a separate shortened NMR tube capped with a septum was placed the hydrosilane precursor in 0.25–0.5 mL of C_7D_8 . The solutions were then cooled in a dry ice/acetone bath (-78 °C unless otherwise noted), and the hydrosilane solution was added by syringe to the NMR tube containing the platinum precursor. After sitting for a few minutes at low temperature, the tube was removed, shaken vigorously for a few seconds, then returned to the cold bath. The sample was then placed in the precooled NMR magnet at the desired temperature, and NMR data were then collected at various reaction times and, in some cases, different temperatures after addition.

Reaction of $(\text{Ph}_3\text{P})_2\text{Pt}(\eta^2\text{-C}_2\text{H}_4)$ (6**) with 10,10-Dihydrophenoxasilin (**1**): Isolation of $[(\text{Ph}_3\text{P})\text{Pt}(\mu\text{-}\eta^2\text{-H-SiC}_2\text{H}_5\text{O})_2]$ (**8**).** **a. Room-Temperature Reaction.** 10,10-Dihydrophenoxasilin (**1**) (25 mg, 0.13 mmol) was reacted with $(\text{Ph}_3\text{P})_2\text{Pt}(\eta^2\text{-C}_2\text{H}_4)$ (**6**) (77 mg, 0.10 mmol) in C_6D_6 (total volume = 1 mL) in an inert atmosphere drybox. Immediately upon addition, gas evolution was observed, which continued for several minutes. After 10 min a golden-yellow solid precipitated from the red-brown solution. After approximately 48 h, the golden-yellow solid was filtered and washed twice with two small portions of C_6D_6 . The solid was dried in vacuo to give **8** (46 mg, 71% yield based on unsolvated **8**).

Characterization Data for 8. $^1\text{H}\{^{31}\text{P}\}$ NMR (500 MHz, $\text{CD}_2\text{-Cl}_2$): δ 7.7–6.9 (ArH), 3.25 (s, $^1J_{\text{PtH}} = 691$, $^2J_{\text{PtH}} = 136$, $\text{Pt}\cdots\text{H}\cdots\text{Si}$). $^{31}\text{P}\{^1\text{H}\}$ NMR (121 MHz, CD_2Cl_2): δ 36.6 (s, $^1J_{\text{PP}} = 4369$, $^2J_{\text{PP}} = 249$, $^3J_{\text{PP}} = 59$). ^1H - ^{29}Si HMQC (500 MHz, $\text{CD}_2\text{-Cl}_2$): correlation observed between ^1H resonance at 3.2 ppm and Si resonance at 128 ppm. IR (solid) (ν , cm^{-1}): 1686 (bridging $\text{Pt}\cdots\text{H}\cdots\text{Si}$). Anal. Calcd for $\text{C}_{60}\text{H}_{50}\text{O}_2\text{P}_2\text{Pt}_2\text{Si}_2$: C, 54.95; H, 3.84. Found: C, 56.54; H, 3.76 (may contain benzene-*d*₆ of solvation, $\text{C}_{60}\text{H}_{50}\text{O}_2\text{P}_2\text{Pt}_2\text{Si}_2\cdot\text{C}_6\text{D}_6$: C, 56.89; H, 3.47).

In a separate experiment, a solution of **1** (23 mg, 0.12 mmol, 1 mL of C_7D_8) was added to **6** (76 mg, 0.10 mmol). Gas evolution was observed immediately. The red-brown reaction mixture was transferred to a NMR tube and data collection begun within 10 min of initial mixing. After 30 min a golden-yellow solid (**8**, 46 mg) was present in the NMR tube.

Selected NMR Data Collected Starting 10 min after Mixing. ^1H NMR (500 MHz, C_7D_8 , 300 K): δ 5.85 (m, tentative assignment, SiH for **9**), 5.36 (br, overlapping with C_2H_4 , SiH for **7**), 5.25 (s, C_2H_4), 5.06 (s, unreacted **1**), 4.50 (s, H_2), -1.86 (br s, $^1J_{\text{PtH}} = 973$, PtH for **7**). $^{31}\text{P}\{^1\text{H}\}$ NMR (202 MHz, C_7D_8 , 300 K): δ 38.7 (s, $^1J_{\text{PP}} = 2134$, tentative assignment, **9**), 30.6 (s, **10**, minor amount), 25.9 (s, OPPh_3), 11.2 (br, covering range 0–20 ppm).

After 20 min the ^1H NMR and ^{31}P spectra were essentially unchanged, but the signals at 5.36 and -1.86 in the proton spectrum had decreased considerably in intensity. After 4 h, the ^{31}P spectrum showed only a minor signal for **9** and a larger resonance for **10**. A broad peak was present at 2.8 ppm (range -5 to 10 ppm). After the golden-yellow solid was removed, the remaining amber solution was analyzed by $^{31}\text{P}\{^1\text{H}\}$ NMR spectroscopy. $^{31}\text{P}\{^1\text{H}\}$ NMR data for the amber solution after removal of **8** (202 MHz, C_7D_8 , 300 K, after 6 days): δ 67.9 (s, minor component, **11**), 30.6 (s, $^1J_{\text{PP}} = 1701$, **10**), 26.5 (OPPh_3), 9.4 (br, range 5–15 ppm). $^{31}\text{P}\{^1\text{H}\}$ NMR data for the amber solution after removal of **8** (202 MHz, C_7D_8 , 183 K, after 6 days): δ 30.5 (br, **10**), 27.9 (b, OPPh_3), 11.7 (s, $^1J_{\text{PP}} = 3819$, $\text{Pt}(\text{PPh}_3)_4$), -6.4 (s, PPh_3).

b. Low-Temperature Reaction. A solution of **1** (16 mg, 0.081 mmol, 0.25 mL C_7D_8) was added to a solution of **6** (58 mg, 0.078 mmol, 0.75 mL of C_7D_8) at 77 K. After a few minutes the tube was transferred to a cold bath at 195 K for approximately 1 min. Then the contents were shaken vigorously for a few seconds. The NMR tube was then transferred to a precooled NMR magnet at 223 K.

(31) (a) Gilman, H.; Zuech, E. A. *J. Org. Chem.* **1959**, *24*, 1394. (b) Gilman, H.; Zuech, E. A. *J. Org. Chem.* **1961**, *26*, 2013. (c) A modified procedure described for the incorporation of a N-Et group was used: Gilman, H.; Zuech, E. A. *J. Org. Chem.* **1961**, *26*, 3481.

Selected NMR Data Collected Just after Mixing. ^1H NMR (500 MHz, C_7D_8 , 223 K): δ 5.41 (m, overlapping with C_2H_4 , SiH for **7**), 5.28 (s, C_2H_4), 4.54 (s, minor component, H_2), 2.69 (s, $^2J_{\text{PH}} = 30$, C_2H_4 for **6**), -1.50 (dd, $^1J_{\text{PIP}} = 973$, $^2J_{\text{PH}} = 156$ (*trans*), 16 (*cis*), PtH for **7**). $^{31}\text{P}\{^1\text{H}\}$ NMR (202 MHz, C_7D_8 , 223 K): δ 34.2 (br s, $^1J_{\text{PIP}} = 1788$, P *trans* to Si for **7**), 34.0 (s, $^1J_{\text{PIP}} = 3714$, **6**), 33.4 (br s, $^1J_{\text{PIP}} = 2422$, P *trans* to H for **7**), 25.9 (s, OPPh_3).

The ^1H and ^{31}P NMR spectra remained unchanged for 3 h at 223 K. After 3 h the temperature was raised to 243 K and the ^1H and ^{31}P NMR spectra obtained were similar to the data collected at 223 K, but the signals for **6** and **7** had broadened. The NMR tube contained a yellow solution (no solid was present at this time) and was quickly removed and shaken, then immediately returned to the precooled magnet. Further broadening of the signals occurred when the temperature was raised to 263 K (4.5 h after mixing) then 283 K (5 h after mixing).

Selected NMR Data Collected 5 h after Mixing. ^1H NMR (500 MHz, C_7D_8 , 283 K): δ 5.43 (s, overlapping with C_2H_4 , SiH for **7**), 5.36 (br, C_2H_4), 4.51 (s, H_2), -1.79 (br s, $^1J_{\text{PH}} = 972$, PtH for **7**). $^{31}\text{P}\{^1\text{H}\}$ NMR (202 MHz, C_7D_8 , 283 K): δ 22 (br, range 5–40 ppm), 24.9 (s, OPPh_3), minor resonances observed between 4 and 17 ppm (unassigned). A minor resonance was also observed at 29.3 (s, **10**).

After 5 h, the NMR tube was again quickly removed and shaken, then immediately returned to the NMR magnet. The tube now contained a yellow solution and a yellow precipitate. The temperature was raised to 303 K after 5.5 h, and the $^{31}\text{P}\{^1\text{H}\}$ NMR spectrum was essentially identical to the data collected at 283 K except for a minor resonance at 66 ppm tentatively assigned to **11**. The ^1H NMR spectrum recorded at 303 K did not show any signals attributable to complex **7**.

After 6.25 h the temperature was lowered to 223 K, then to 183 K. $^{31}\text{P}\{^1\text{H}\}$ NMR data collected 6.25 h after mixing (202 MHz, C_7D_8 , 223 K): δ 65.5 (s, minor component, **11**), 29.7 (s, minor component, **10**), 25.9 (s, OPPh_3), 5 (br, range -15 to 40 ppm), several unassigned minor resonance observed between 4 and 25 ppm. $^{31}\text{P}\{^1\text{H}\}$ NMR data collected 6.75 h after mixing (202 MHz, C_7D_8 , 183 K): δ 26.1 (s, OPPh_3), 10.3 (s, $^1J_{\text{PIP}} = 3833$, $\text{Pt}(\text{PPh}_3)_4$),²⁰ -7.8 (s, PPh_3).

c. High-Temperature Reaction. A solution of **1** (27 mg, 0.14 mmol, 0.25 mL of C_7D_8) was added to a solution of **6** (97 mg, 0.13 mmol, 0.75 mL of C_7D_8) at room temperature. Then the NMR tube containing the reaction mixture was immediately placed in a preheated NMR magnet at 323 K. Selected NMR data collected 5 min after mixing: ^1H NMR (500 MHz, C_7D_8 , 323 K): δ 5.18 (br s, C_2H_4), 4.49 (s, H_2), 3.21 (s, $^1J_{\text{PH}} = 682$, $^2J_{\text{PH}} = 128$, $\text{Pt}\cdots\text{H}\cdots\text{Si}$ for **8**). $^{31}\text{P}\{^1\text{H}\}$ NMR (202 MHz, C_7D_8 , 323 K): δ 68.3 (s, $^1J_{\text{PIP}} = 3454$, $^2J_{\text{PIP}} = 466$, $^3J_{\text{PP}} = 76$, **11**), 30.6 (s, $^1J_{\text{PIP}} = 1625$, **10**), 30 (br, range 5–50 ppm), 25.6 (s, OPPh_3). Some minor unassigned resonances were observed between 10 and 40 ppm.

In a similar experiment, a solution of **1** (40 mg, 0.20 mmol, 0.10 mL of C_7D_8) was added to a solution of **6** (146 mg, 0.20 mmol, 1.0 mL of C_7D_8) at room temperature. Then the NMR tube containing the reaction mixture was immediately placed in a preheated NMR magnet at 323 K. After NMR data collection, a light golden solid (**8**) was observed in the tube (92 mg crude yield, 72% based on Pt).

Selected $^{31}\text{P}\{^1\text{H}\}$ NMR (202 MHz, C_7D_8 , 183 K, 7 h after mixing): δ 26.1 (s, OPPh_3), 10.3 (s, $\text{Pt}(\text{PPh}_3)_4$), -7.8 (s, PPh_3). $^{195}\text{Pt}\{^1\text{H}\}$ NMR (107 MHz, C_7D_8 , 300 K, 9 h after addition): δ -4375 (m). The trinuclear complex **11** was not isolated from the reaction mixture due to the difficulty in separation of the low yield of material in the presence of a significant amount of PPh_3 and $\text{Pt}(\text{PPh}_3)_4$ as well as other minor impurities.

Reaction of $(\text{Ph}_3\text{P})_2\text{Pt}(\eta^2\text{-C}_2\text{H}_4)$ (6**) with 2,8-Dimethyl-10,10-dihydrophenoxasilin (**2**): Isolation of $[(\text{Ph}_3\text{P})\text{Pt}(\mu\text{-SiC}_{14}\text{H}_{12}\text{O})_3]$ (**16**). a. Room-Temperature Reaction.** A solution of 2,8-dimethyl-

10,10-dihydrophenoxasilin (**2**) (25 mg, 0.11 mmol) dissolved in C_7D_8 (0.25 mL) was added to an NMR tube containing a solution of $(\text{Ph}_3\text{P})_2\text{Pt}(\eta^2\text{-C}_2\text{H}_4)$ (**6**) (83 mg, 0.11 mmol) in C_7D_8 (0.75 mL). A small amount of gas evolution was observed, and the tube was shaken for about 10 s to thoroughly mix the contents, providing a reddish-amber solution. NMR experiments were begun within 10 min of initial mixing.

Selected NMR Data Collected 10 min after Mixing. ^1H NMR (500 MHz, C_7D_8 , 300 K): δ 5.83 (m, SiH, minor component, tentative assignment, **13**), 5.25 (s, C_2H_4), 5.13 (s, minor amount of unreacted **2**), 4.50 (s, H_2), 0.36 (br, $^1J_{\text{PH}} \approx 640$, PtH for **15**), -1.8 (br s, minor component, $^1J_{\text{PH}} \approx 980$ Hz, tentative assignment, **12**). $^{31}\text{P}\{^1\text{H}\}$ NMR (202 MHz, C_7D_8 , 300 K): δ 29.2 (s, minor component, tentative assignment, **14**), 24.3 (s, OPPh_3), 19.2 (br, covering range 12–25 ppm).

Selected NMR Data Collected 45 min after Mixing. $^{31}\text{P}\{^1\text{H}\}$ NMR (C_7D_8 , 202 MHz, 300 K): δ 68.7 (s, **16**), 29.2 (s, $^1J_{\text{PIP}} = 1621$, tentative assignment, **14**), 24.3 (s, OPPh_3), 18.9 (br, range 12–25 ppm). The proton and phosphorus NMR spectra remained essentially unchanged until approximately 3.5 h after mixing, when the temperature was lowered to approximately 223 K.

Selected NMR Data Collected 3.5 h after Mixing. ^1H NMR (500 MHz, C_7D_8 , 225 K): δ 5.29 (s, C_2H_4), 4.55 (s, H_2), 2.71 (br, tentative assignment, $\text{Pt}\cdots\text{H}\cdots\text{Si}$ for **15**), -5.04 (br s, $^1J_{\text{PH}} = 544$ Hz, Pt–H for **15**). $^{31}\text{P}\{^1\text{H}\}$ NMR (C_7D_8 , 202 MHz, 225 K): δ 68.9 (s, **16**), 30.2 (br, $\text{Pt}(\text{PPh}_3)$ for **15**), 28.9 (s, **14**), 25.1 (s, OPPh_3), 20.3 (br, $\text{Pt}(\text{PPh}_3)_2$ for **15**), -5 (br, PPh_3).

After 4 h the temperature was warmed to 300 K and the ^1H and ^{31}P NMR spectra looked essentially identical to the data collected at room temperature approximately 1 h after mixing. After 6 days, NMR measurements were again obtained on the reaction solution. No solid was present in the NMR tube.

Selected NMR Data Collected 6 days after Mixing. $^{31}\text{P}\{^1\text{H}\}$ NMR (202 MHz, C_7D_8 , 300 K): δ 68.7 (s, $^1J_{\text{PIP}} = 3475$, $^1J_{\text{PIP}} = 466$, $^3J_{\text{PP}} = 76$, **16**, major component), 29.2 (s, $^1J_{\text{PIP}} = 1623$ Hz, **14**), 24.3 (s, OPPh_3), 15.0 (br, **15**). ^1H NMR (500 MHz, C_7D_8 , 223 K): δ 5.29 (s, C_2H_4), -5.04 (br s, $^1J_{\text{PH}} = 544$, PtH for **15**). $^{31}\text{P}\{^1\text{H}\}$ NMR (202 MHz, C_7D_8 , 223 K): δ 68.7 (s, **16**), 30.3 (t, $^1J_{\text{PIP}} = 4081$, $^2J_{\text{PIP}} = 198$, $^3J_{\text{PP}} = 27$, $\text{Pt}(\text{PPh}_3)$ for **15**), 28.9 (s, **14**), 25.2 (s, OPPh_3), 20.3 (d, $^1J_{\text{PIP}} = 3504$, $^3J_{\text{PP}} = 27$, $\text{Pt}(\text{PPh}_3)_2$ for **15**). $^{31}\text{P}\{^1\text{H}\}$ NMR (202 MHz, C_7D_8 , 183 K): δ 68.9 (br, $^1J_{\text{PIP}} = 3425$, **16**), 30.3 (br, **15**), 28.6 (br, **14**), 25.4 (s, OPPh_3), 20.2 (br, **15**), 10.2 (s, $^1J_{\text{PIP}} = 3841$, $\text{Pt}(\text{Ph}_3\text{P})_4$), -7.9 (s, PPh_3).

Two weeks after initial mixing, additional NMR experiments were performed on the reaction solution. No solid was observed in the solution. $^{29}\text{Si}\{^1\text{H}\}$ NMR (99 MHz, C_7D_8 , 300 K): δ 244.6 (s, $^1J_{\text{PSi}} = 977$, **16**). $^{195}\text{Pt}\{^1\text{H}\}$ (108 MHz, C_7D_8 , 300 K): δ -4353 (m).

Approximately 3 months after initial mixing, evaporation of the solvent provided glassy dark X-ray-quality red crystals (92 mg) of **16** (contains 2.5 molecules of toluene-*d*₈ solvate). NMR spectroscopic data for **16**: $^{31}\text{P}\{^1\text{H}\}$ (202 MHz, C_7D_8 , 300 K): δ 68.7 (s, $^1J_{\text{PIP}} = 3474$, $^2J_{\text{PIP}} = 466$, $^3J_{\text{PP}} = 76$). $^{29}\text{Si}\{^1\text{H}\}$ (99 MHz, C_7D_8 , 300 K): δ 239.6 (s, $^1J_{\text{SiPt}} = 976$). $^{195}\text{Pt}\{^1\text{H}\}$ NMR (107 MHz, C_7D_8 , 300 K): δ -4352 (m). The sample contains an OPPh_3 impurity.

b. Low-Temperature Reaction. A solution of 2,8-dimethyl-10,10-dihydrophenoxasilin (**2**) (25 mg, 0.11 mmol) dissolved in C_7D_8 (0.25 mL) was added to an NMR tube containing a solution of $(\text{Ph}_3\text{P})_2\text{Pt}(\eta^2\text{-C}_2\text{H}_4)$ (**6**) (83 mg, 0.11 mmol) in C_7D_8 (0.75 mL) at 77 K. After several minutes the NMR tube was placed in a 195 K bath for approximately 5 min. The tube was then shaken vigorously, then placed in a precooled magnet at 223 K. NMR data collection was begun within 5 min, and after ~2.5 h, the temperature was raised from 223 to 303 K, in 20 K increments over a 2 h period. NMR data collection was performed at each temperature.

Selected NMR Data Collected 5–10 min after Mixing. ^1H NMR (500 MHz, C_7D_8 , 223 K): δ 5.59 (m, Si–H for **12**), 5.29 (s,

C_2H_4), 5.1 (br s, possibly unreacted **2**), 4.55 (s, H_2), 2.67 (s, $^2J_{\text{PtH}} = 30$, C_2H_4 for unreacted **6**), -1.48 (dd, $^1J_{\text{PtH}} = 977$, $^2J_{\text{PH}} = 154$ (*trans*), 19 (*cis*), PtH for **12**). $^{31}\text{P}\{^1\text{H}\}$ NMR (202 MHz, C_7D_8 , 223 K): δ 33.9 (s, $^1J_{\text{PP}} = 3712$, unreacted **6**), 33.3 (resonance probably overlapping with unreacted **6**, $^1J_{\text{PP}} = 1761$, P *trans* to Si for **12**), 33.2 (d, $^1J_{\text{PP}} = 2439$, $^2J_{\text{PP}} = 11$, P *trans* to H for **12**), 25.4 (s, OPPh_3).

Selected NMR Data Collected 2.75 h after Mixing. ^1H NMR (500 MHz, C_7D_8 , 243 K): 5.61 (br m, SiH for **12**), 5.47 (t, unassigned), 5.28 (s, C_2H_4), 4.62 (m, unassigned minor component), 4.54 (s, H_2), 2.64 (s, unreacted **6**), -1.58 (br d, $^1J_{\text{PtH}} = 975$, $^2J_{\text{PH}} = 143$ (*trans*), PtH for **12**), -1.69 (dd, probable PtH, unassigned minor component, $^2J_{\text{PH}} = 155$, 24). $^{31}\text{P}\{^1\text{H}\}$ NMR (202 MHz, C_7D_8 , 243 K): δ 34.2 (unreacted **6**), 33.8 (br s, $^1J_{\text{PP}} = 1754$, **12**), 33.5 (br s, $^1J_{\text{PP}} = 2453$, **12**), 32.9 (br, unidentified minor component), 25.2 (s, OPPh_3).

Selected NMR Data Collected 3.25 h after Mixing. ^1H NMR (500 MHz, C_7D_8 , 263 K): δ 5.68 (br s, $^2J_{\text{PtH}} = 64$, SiH for **12**), 5.46 (t, $J = 49$, unassigned), 5.27 (br s, C_2H_4), 4.59 (t, $J = 27$, unassigned), 4.52 (s, H_2), 2.58 (br, **6**), -1.68 (br d, $^1J_{\text{PtH}} = 978$, $^2J_{\text{PH}} = 133$, PtH for **12**). $^{31}\text{P}\{^1\text{H}\}$ NMR (202 MHz, C_7D_8 , 263 K): δ 34.3 (br, **6**), 33.7 (br, $^1J_{\text{PP}} = 2326$, **12**), 32.7 (s, $^1J_{\text{PP}} = 1777$, **12**), 24.9 (s, OPPh_3).

Selected NMR Data Collected 3.75 h after Mixing. ^1H NMR (500 MHz, C_7D_8 , 283 K): δ 5.60 (minor component, **12**), 5.46 (minor component, unassigned), 5.25 (br s, C_2H_4), 4.61 (t, minor component, unassigned), 4.51 (s, H_2), -1.77 (br s, $^1J_{\text{PtH}} = 973$, **12**), -7.71 (d, $^1J_{\text{PtH}} = 729$, $J_{\text{PH}} = 16$, PtH, unassigned minor component). $^{31}\text{P}\{^1\text{H}\}$ NMR (202 MHz, C_7D_8 , 283 K): δ 32.7 (s, minor component, unassigned), 24.7 (s, OPPh_3), 25.0 (br, range 0–50 ppm), 4.2 (s, minor component, unassigned).

The ^1H NMR data collected at 303 K (5 h after mixing) were essentially the same as the ^1H NMR data collected at 283 K listed above, but the Si-H and Pt-H resonances had almost disappeared. $^{31}\text{P}\{^1\text{H}\}$ NMR (202 MHz, C_7D_8 , 303 K, 5 h after mixing): δ 68.7 (s, minor component, **16**), 29.2 (s, minor component, **14**), 24.5 (s, OPPh_3), 22.2 (br, range 0–50 ppm).

After the NMR experiments were completed, pentane (~3 mL) was added to the reaction solution and the NMR tube was placed in a freezer at -40 °C for several weeks. An orange-red solid was observed. ^{31}P NMR spectroscopic data of the solid dissolved in C_7D_8 at room temperature and -50 °C showed the presence of several components. Resonances for **14** (minor component), **15** (major component), **16** (minor component), OPPh_3 , and PPh_3 were observed in the ^{31}P NMR spectra (for δ and J values see above). Complexes **14**–**16** were not isolated from the reaction mixture.

Reaction of $(\text{Ph}_3\text{P})_2\text{Pt}(\eta^2\text{-C}_2\text{H}_4)$ (6**) with 5-Methyl-10,10-dihydrophenazasiline (**3**): Isolation of $[(\text{Ph}_3\text{P})\text{Pt}(\mu\text{-}\eta^2\text{-H-SiC}_{13}\text{H}_{12}\text{N})_2]$ (**22**).** **a. Low-Temperature Reaction.** A solution of 5-methyl-10,10-dihydrophenazasiline (**3**) (15 mg, 0.071 mmol) in C_7D_8 (approximately 0.25 mL) was added to a solution of $(\text{Ph}_3\text{P})_2\text{Pt}(\eta^2\text{-C}_2\text{H}_4)$ (**6**) (53 mg, 0.071 mmol) in C_7D_8 (~0.75 mL) cooled in a liquid N_2 bath (77 K). The tube was then placed in a dry ice/acetone bath (195 K). Once the solution had melted, the reaction tube was shaken several times to mix the contents. The tube was then placed in a precooled NMR magnet (223 K), and NMR experiments were begun within 5 min.

Selected NMR Data Collected 5 min after Mixing. ^1H NMR (500 MHz, C_7D_8 , 223 K): δ 5.29 (s, C_2H_4), 4.86 (m, SiH for **17**), 2.70 (s, $^2J_{\text{PtH}} = 60$, C_2H_4 for **6**), -1.28 (dd, $^1J_{\text{PtH}} = 988$, $^2J_{\text{PH}} = 156$ (*trans*), 20 (*cis*), PtH for **17**). $^{31}\text{P}\{^1\text{H}\}$ NMR (202 MHz, C_7D_8 , 223 K): δ 36.6 (d, $^1J_{\text{PP}} = 1818$, $^2J_{\text{PSi}} = 153$, $^2J_{\text{PP}} = 10$, P *trans* to Si for **17**), 35.2 (d, $^1J_{\text{PP}} = 2447$, $^2J_{\text{PP}} = 10$, P *trans* to H for **17**), 34.0 (s, $^1J_{\text{PP}} = 3714$, unreacted **6**), 25.8 (s, OPPh_3). The spectra remained unchanged almost 2 h after mixing.

Selected NMR Data Collected 2 h after Mixing. ^1H NMR (500 MHz, C_7D_8 , 243 K): δ 5.28 (s, C_2H_4), 4.85 (m, SiH for **17**), 4.54

(s, minor component, H_2), 2.64 (s, **6**), -1.38 (dd, $^1J_{\text{PtH}} = 987$, $^2J_{\text{PH}} = 156$ (*trans*), 19 (*cis*), PtH for **17**). $^{31}\text{P}\{^1\text{H}\}$ NMR (202 MHz, C_7D_8 , 243 K): δ 36.4 (br s, $^1J_{\text{PP}} = 1808$, **17**), 35.4 (br s, $^1J_{\text{PP}} = 2456$, **17**), 34.2 (s, $^1J_{\text{PP}} = 3723$, unreacted **6**), 25.6 (s, OPPh_3).

Selected NMR Data Collected 2.75 h after Mixing. ^1H NMR (500 MHz, C_7D_8 , 263 K): δ 5.27 (s, C_2H_4), 4.85 (br s, SiH for **17**), 4.53 (s, minor component, H_2), 2.59 (br, **6**), -1.47 (br d, $^1J_{\text{PtH}} = 985$, $^2J_{\text{PH}} = 152$ (*trans*), PtH for **17**). $^{31}\text{P}\{^1\text{H}\}$ NMR (202 MHz, C_7D_8 , 263 K): δ 35.5 (br, **17**), 34.4 (s, $^1J_{\text{PP}} = 3733$, unreacted **6**), 25.6 (s, OPPh_3).

Selected NMR Data Collected 4 h after Mixing. ^1H NMR (500 MHz, C_7D_8 , 283 K): δ 5.26 (br s, C_2H_4), 4.85 (br m, SiH for **17**), 4.51 (s, H_2), 2.59 (br, **6**), -1.56 (br s, $^1J_{\text{PtH}} = 987$, PtH for **17**). $^{31}\text{P}\{^1\text{H}\}$ NMR (202 MHz, C_7D_8 , 283 K): δ 32 (br, range 15–50 ppm), 24.7 (s, OPPh_3). Several minor unassigned resonances were observed between 5 and 40 ppm.

Selected NMR Data Collected 5.5 h after Mixing. $^{31}\text{P}\{^1\text{H}\}$ NMR (202 MHz, C_7D_8 , 303 K): δ 66.2 (s, minor component, **21**), 29.8 (s, $^1J_{\text{PP}} = 1628$, **19**), 28 (br, range 0–50 ppm), 24.5 (s, OPPh_3). Several minor unassigned resonances were observed between 0 and 30 ppm. No hydride resonances for **17** were observed in the ^1H NMR spectrum at 303 K.

After 24 h the NMR tube contained an orange solution and a yellow solid (**22**). The soluble fraction was found to contain a mixture of unreacted **6**, OPPh_3 , and $\text{Pt}(\text{PPh}_3)_4$ along with a minor amount of **21** and PPh_3 .

Selected NMR Data Collected 24 h after Mixing. $^{31}\text{P}\{^1\text{H}\}$ NMR (202 MHz, C_7D_8 , 223 K): δ 65.7 (s, minor component, **21**), 34.0 (br s, **6**), 29.7 (s, **19**), 25.6 (s, OPPh_3), 25 (br, range -10 to 50 ppm). Several minor unassigned resonances were observed between 0 and 25 ppm. $^{31}\text{P}\{^1\text{H}\}$ NMR (202 MHz, C_7D_8 , 183 K): δ 33.5 (s, **6**), 25.7 (s, OPPh_3), 10.2 (s, $^1J_{\text{PP}} = 3834$, Pt (PPh_3)₄), -7.8 (s, minor component, PPh_3).

b. Room-Temperature Reaction. A solution of 5-methyl-10,10-dihydrophenazasiline (**3**) (15 mg, 0.071 mmol) dissolved in C_7D_8 (0.25 mL) was added to a solution of $(\text{Ph}_3\text{P})_2\text{Pt}(\eta^2\text{-C}_2\text{H}_4)$ (**6**) (53 mg, 0.071 mmol) in C_7D_8 (0.75 mL). Gas evolution was observed, the mixture was transferred to a NMR tube, and NMR experiments were begun within 10 min of initial mixing.

Selected NMR Data Collected 10 min after Mixing. ^1H NMR (500 MHz, C_7D_8 , 300 K): δ 5.25 (br s, C_2H_4), 4.86 (br s, tentative assignment, SiH for **17**), 4.50 (s, H_2), -1.64 (br s, $^1J_{\text{PtH}} = 990$, PtH for **17**). $^{31}\text{P}\{^1\text{H}\}$ NMR (202 MHz, C_7D_8 , 300 K): δ 66.2 (s, minor component, **21**), 37.9 (s, tentative assignment, minor component, **18**), 29.9 (s, $^1J_{\text{PP}} = 1630$, minor component, **19**), 24.8 (s, minor component, unassigned), 24.3 (s, OPPh_3), 22 (br, range 10–40 ppm). The ^1H NMR spectrum was essentially the same at 1.5 and 3 h after mixing, but the peaks at 4.86 and -1.64 eventually disappeared and a new broad region was present near 0 ppm that was tentatively assigned to an averaged $\text{Pt}\cdots\text{H}\cdots\text{Si}$ signal for **20**. The $^{31}\text{P}\{^1\text{H}\}$ NMR spectrum was similar after 1.5 and 3 h, but the signal at 37.9 ppm eventually disappeared.

Selected NMR Data Collected 4.5 h after Mixing. ^1H NMR (500 MHz, C_7D_8 , 223 K): δ 5.29 (s, C_2H_4), 4.55 (s, H_2), -5.98 (br s, $^1J_{\text{PtH}} \approx 570$, PtH for **20**). $^{31}\text{P}\{^1\text{H}\}$ NMR (202 MHz, C_7D_8 , 223 K): δ 65.7 (s, $^1J_{\text{PP}}$ not resolved, $^2J_{\text{PP}} = 491$, $^3J_{\text{PP}} = 74$, **21**), 30.7 (br s, $^1J_{\text{PP}} = 4174$, $^2J_{\text{PP}} = 278$, PtPPh_3 for **20**), 29.7 (s, minor component, **19**), 25.1 (s, OPPh_3), 18.6 (br s, $^1J_{\text{PP}} = 3666$, Pt(PPh_3)₂ for **20**). ($\text{Pt}\cdots\text{H}\cdots\text{Si}$ for **20** not located/observed.)

Selected NMR Data Collected 6 h after Mixing. $^{31}\text{P}\{^1\text{H}\}$ NMR (202 MHz, C_7D_8 , 183 K): δ 65.5 (s, minor component, **21**), 31.9 (br s, $^1J_{\text{PP}} = 4088$, $^2J_{\text{PP}} = 298$, PtPPh_3 for **20**), 25.5 (s, OPPh_3), 18.6 (br s, $^1J_{\text{PP}} = 3652$, Pt(PPh_3)₂ for **20**), 10.2 (s, $^1J_{\text{PP}} = 3831$, Pt(PPh_3)₄), -7.8 (s, PPh_3).

After 24 h, a yellow crystalline solid was observed in the NMR tube along with a red solution. X-ray crystallography revealed the

structure of the yellow solid to be that of the symmetrical dimer **22**. The structure also contained one molecule of C_7D_8 .

In a similar experiment, 10,10-dihydrophenazasiline (**3**) (11 mg, 0.052 mmol) dissolved in C_7D_8 (0.25 mL) was added to a solution of $(Ph_3P)_2Pt(\eta^2-C_2H_4)$ (**6**) (40 mg, 0.054 mmol) in C_7D_8 (0.50 mL). After 48 h, yellow microcrystalline **22** was observed (22 mg, 55% based on **22**· C_7D_8). 1H NMR (500 MHz, CD_2Cl_2 , 300 K): δ 7.38–6.55 (ArH), 3.26 (s, NMe), 2.36 (s, Pt satellites not resolved, tentative assignment, $Pt\cdots H\cdots Si$). $^{31}P\{^1H\}$ NMR (202 MHz, CD_2Cl_2 , 300 K): δ 36.9 (s, $^1J_{PtP} = 4349$, $^2J_{PtP} = 265$, $^3J_{PtP} = 60$). IR (solid, cm^{-1}): 1687 ($Pt\cdots H\cdots Si$). Anal. Calcd for $C_{61}H_{54}N_2P_2Si_2Pt_2\cdot C_7D_8$: C, 57.73; H, 4.92. Found: C, 57.63; H, 4.33.

c. High-Temperature Reaction. A solution of 5-methyl-10,10-dihydrophenazasiline (**3**) (25 mg, 0.12 mmol) in C_7D_8 (~0.25 mL) was added to a solution of $(Ph_3P)_2Pt(\eta^2-C_2H_4)$ (**6**) (90 mg, 0.12 mmol) in C_7D_8 (~1 mL). Vigorous gas evolution was observed immediately upon addition, and the solution turned a red-amber color. The tube was shaken to mix the contents, then placed in a preheated (50 °C) NMR magnet. NMR data collection was begun within a few minutes.

Selected NMR Data Collected 5 min after Mixing. The 1H NMR data collected at 323 K were essentially the same as the data for the room-temperature reaction collected just after mixing, but there were no resolved hydride resonances observed. $^{31}P\{^1H\}$ NMR (202 MHz, C_7D_8 , 323 K): δ 66.4 (s, $^1J_{PtP} = 3528$, $^2J_{PtP} = 490$, $^3J_{PtP} = 76$, **21**), 29.9 (s, $^1J_{PtP} = 1622$, **19**), 29.0 (br s, minor component, unassigned), 24.2 (s, $OPPh_3$), 24 (br, range 10–40 ppm). Several small unassigned peaks were observed between 6 and 14 ppm. The spectra remained unchanged 1.5 h after mixing.

Selected NMR Data Collected 2.5 h after Mixing. 1H NMR (500 MHz, C_7D_8 , 223 K): δ 5.29 (s, C_2H_4), 4.55 (s, H_2), –6.01 (br s, $^1J_{PtH} = 590$, minor component, Pt–H for **20**). $^{31}P\{^1H\}$ NMR (202 MHz, C_7D_8 , 223 K): δ 65.7 (s, $^1J_{PtP} = 3467$, $^2J_{PtP} = 490$, $^3J_{PtP} = 77$, **21**), 37.6 (d, minor component, **18**), 29.7 (s, **19**), 25.3 (s, $OPPh_3$), 18.6 (br s, unassigned), 10 (br, range –15 to 45, unsymmetrical). Several small unassigned peaks were observed between 3 and 50 ppm ($Pt\cdots H\cdots Si$ for **20** not located/observed).

Selected NMR Data Collected 3.5 h after Mixing. $^{31}P\{^1H\}$ NMR (202 MHz, C_7D_8 , 183 K): δ 65.5 (s, minor component, **21**), 25.5 (s, $OPPh_3$), 10.2 (s, $^1J_{PtP} = 3838$, $Pt(PPh_3)_4$), –7.8 (s, PPh_3).

Selected NMR Data Collected 6 h after Mixing. $^{29}Si\{^1H\}$ NMR (99 MHz, C_7D_8 , 300 K): δ 254.6 (s, $^1J_{PtSi} = 964$, **21**).

Reaction of $(Ph_3P)_2Pt(\eta^2-C_2H_4)$ (6**) with 2,5,8-Trimethyl-10,10-dihydrophenazasiline (**4**). a. Low-Temperature Reaction.** A solution of 2,5,8-trimethyl-10,10-dihydrophenazasiline (**4**) (20 mg, 0.084 mmol) in C_7D_8 (approximately 0.25 mL) was added to a cooled solution of $(Ph_3P)_2Pt(\eta^2-C_2H_4)$ (**6**) (63 mg, 0.084 mmol) in C_7D_8 (~0.75 mL) at 77 K. After the mixture had frozen, the tube was placed in a –78 °C bath for ca. 2 min before it was removed, shaken to mix contents, and placed into a precooled NMR magnet at 223 K. Gas evolution was observed in the reaction solution. NMR experiments were begun within about 5 min of mixing (precursor **4** was consumed, but some of **6** remained).

Selected NMR Data Collected 5–10 min after Mixing. 1H NMR (500 MHz, C_7D_8 , 223 K): δ 5.29 (s, C_2H_4), 4.96 (m, SiH for **23**), 4.55 (s, minor component, H_2), 2.69 (s, C_2H_4 for **6**), –1.31 (dd, $^1J_{PtH} = 996$, $^2J_{PtH} = 155$ (*trans*), 21 (*cis*), PtH for **23**). $^{31}P\{^1H\}$ NMR (202 MHz, C_7D_8 , 223 K): δ 35.7 (d, $^1J_{PtP} = 1798$, $^2J_{PtP} = 10$, P *trans* to Si for **23**), 35.3 (d, $^1J_{PtP} = 2455$, $^2J_{PtP} = 10$, P *trans* to H for **23**), 34.0 (s, $^1J_{PtP} = 3714$, **6**), 25.7 (s, $OPPh_3$). The 1H and $^{31}P\{^1H\}$ NMR spectra remained unchanged after 1 h at 223 K.

Selected NMR Data Collected 2 h after Mixing. The 1H NMR data (243 K) were essentially identical to the data collected at earlier time intervals at 223 K, but the hydride resonances for **23** were slightly broadened. The $^{31}P\{^1H\}$ NMR data (243 K) were also similar to the data collected earlier in the reaction at 223 K, but

the resonances for **23** were now broader and the doublet pattern was no longer visible.

Selected NMR Data Collected 3 h after Mixing. 1H NMR (500 MHz, C_7D_8 , 263 K): δ 5.27 (br s, C_2H_4), 4.96 (br, SiH for **23**), 4.53 (s, H_2), 2.59 (br s, C_2H_4 for **6**), –1.47 (br d, $^1J_{PtH} = 993$, $^2J_{PtH} = 152$ (*trans*), PtH for **23**). $^{31}P\{^1H\}$ NMR (202 MHz, C_7D_8 , 263 K): δ 50.4 (br, $Pt(PPh_3)_3$), 35.5 (br, **23**), 34.4 (s, **6**), 24.9 (s, $OPPh_3$).

Selected NMR Data Collected 4 h after Mixing. 1H NMR (500 MHz, C_7D_8 , 283 K): δ 5.26 (br, C_2H_4), 4.96 (m, minor component, SiH for **23**), 4.51 (s, H_2), 2.6 (br, C_2H_4 for **6**), –1.54 (br, PtH for **23**). $^{31}P\{^1H\}$ NMR (202 MHz, C_7D_8 , 283 K): δ 40 (br, range –5–70 ppm), 34.6 (br, $^1J_{PtP} = 3723$, **6**), 29.7 (s, minor component, **25**), 24.6 (s, $OPPh_3$).

Selected NMR Data Collected 4.5 h after Mixing. The 1H NMR data (303 K) did not exhibit hydride resonances for **23** or other complexes. The $^{31}P\{^1H\}$ NMR data (303 K) were similar to the data collected at 4 h (283 K), but the signal at 34 ppm was broader. In addition, two minor resonances were present at 67.4 (s, **27**) and 51.3 (unassigned).

Selected NMR Data Collected 5 h after Mixing. 1H NMR (500 MHz, C_7D_8 , 223 K): δ 5.29 (br s, C_2H_4), 4.55 (s, H_2), –6.06 (t, $^1J_{PtH} = 565$, $^2J_{PtH} = 13$, PtH for **26**). $^{31}P\{^1H\}$ NMR (202 MHz, C_7D_8 , 223 K): δ 66.9 (s, minor component, **27**), 34.0 (s, **6**), 30.2 (t, $^1J_{PtP} = 4058$, $^2J_{PtP} = 253$, $^3J_{PtP} = 28$, $PtPPh_3$ for **26**), 28.5 (s, minor component, **25**), 25.6 (s, $OPPh_3$), 19.4 (d, $^1J_{PtP} = 3682$, $^3J_{PtP} = 29$, $Pt(PPh_3)_2$ for **26**).

Selected NMR Data Collected 5 h after Mixing. $^{13}C\{^1H\}$ NMR (202 MHz, C_7D_8 , 183 K): δ 33.5 (s, **6**), 30.5 (br, **26**), 24.4 (s, $OPPh_3$), 19.4 (br, **26**), 10.2 (s, $^1J_{PtP} = 3829$, $Pt(PPh_3)_4$).

The major Pt–Si-containing product **26** from the reaction could not be isolated in pure form from the complex reaction mixture. (Some of unreacted **6** remained, but **4** was not present.)

b. Room-Temperature Reaction. A solution of 2,5,8-trimethyl-10,10-dihydrophenazasiline (**4**) (26 mg, 0.11 mmol) dissolved in C_7D_8 (0.25 mL) was added to a solution of $(Ph_3P)_2Pt(\eta^2-C_2H_4)$ (**6**) (73 mg, 0.098 mmol) in C_7D_8 (0.75 mL). Gas evolution was observed immediately, the mixture was transferred to a NMR tube, and NMR experiments were begun within 15 min of initial mixing.

Selected NMR Data Collected 15 min after Mixing. 1H NMR (500 MHz, C_7D_8 , 300 K): δ 5.24 (br s, C_2H_4), 4.50 (s, H_2), –0.2 (br s, tentative assignment, averaged $Pt\cdots H\cdots Si$ for **23**). $^{31}P\{^1H\}$ NMR (202 MHz, C_7D_8 , 300 K): δ 67.4 (s, $^1J_{PtP}$ not resolved, minor component, **27**), 38.3 (s, $^1J_{PtP}$ not resolved, minor component, **24**), 29.8 (s, $^1J_{PtP} = 1626$, **25**), 26 (br, range 10–50 ppm), 24.4 (s, $OPPh_3$). Several minor unassigned resonances were observed between 3 and 45 ppm. The 1H and $^{31}P\{^1H\}$ NMR spectra were essentially the same 1 h after mixing, but several of the minor resonances in the ^{31}P spectrum were now absent.

Selected NMR Data Collected 1.5 h after Mixing. 1H NMR (500 MHz, C_7D_8 , 223 K): δ 5.29 (br s, C_2H_4), 4.55 (s, H_2), –6.05 (br t, $^1J_{PtH} = 568$, $^2J_{PtH} \approx 13$, PtH for **26**). $^{31}P\{^1H\}$ NMR (202 MHz, C_7D_8 , 223 K): δ 66.9 (s, minor component, **27**), 30.2 (t, $^1J_{PtP} = 4051$, $^2J_{PtP} = 282$, $^3J_{PtP} = 28$, $PtPPh_3$ for **26**), 29.6 (s, **25**), 25.3 (s, $OPPh_3$), 19.4 (d, $^1J_{PtP} = 3676$, $^3J_{PtP} = 29$, $Pt(PPh_3)_2$ for **26**). A broadened baseline region was observed between –10 and 45 ppm. Several minor unassigned resonances were also observed between 5 and 40 ppm.

Selected NMR Data Collected 2.5 h after Mixing. $^{31}P\{^1H\}$ NMR (202 MHz, C_7D_8 , 183 K): δ 30.4 (br, **26**), 28.4 (br, **25**), 25.6 (s, $OPPh_3$), 19.3 (br, **26**), 10.2 (s, $^1J_{PtP} = 3838$, $Pt(PPh_3)_4$), –7.8 (s, PPh_3).

The room-temperature 1H and $^{31}P\{^1H\}$ NMR spectra taken after 3.25 h were essentially unchanged from the room-temperature data collected between 15 min and 1 h.

Selected NMR Data Collected 2 days after Mixing. $^{31}P\{^1H\}$ NMR (202 MHz, C_7D_8 , 300 K): δ 67.4 (s, $^1J_{PtP} = 3495$, $^2J_{PtP} = 494$, $^3J_{PtP} = 76$, **27**), 29.5 (s, **25**), 28 (br, range 0–50 ppm), 24.4

(s, OPPh_3). $^{31}\text{P}\{\text{H}\}$ NMR (202 MHz, C_7D_8 , 183 K): δ 67.1 (m, minor component, **27**), 33.5 (s, $^1J_{\text{PtP}} = 3696$, minor component, tentative assignment, **6**), 30.4 (br m, **26**), 28.4 (br, **25**), 25.6 (s, OPPh_3), 19.3 (br, **26**), 10.2 (s, $\text{Pt}(\text{PPh}_3)_4$), -7.8 (s, PPh_3). (The $\text{Pt}\cdots\text{H}\cdots\text{Si}$ resonance for **26** was not observed/located.)

Reaction of $(\text{Ph}_3\text{P})_2\text{Pt}(\eta^2\text{-C}_2\text{H}_4)$ (6**) with 2,8-Dibromo-5-methyl-10,10-dihydrophenazasiline (**5**). Isolation of $[(\text{Ph}_3\text{P})_2(\text{H})\text{-Pt}(\mu\text{-SiC}_{13}\text{H}_9\text{Br}_2\text{N})(\mu\text{-}\eta^2\text{-H-SiC}_{13}\text{H}_9\text{Br}_2\text{N})\text{Pt}(\text{PPh}_3)]$ (**30**). a. **Low-Temperature Reaction.** A solution of 2,8-dibromo-5-methyl-10,10-dihydrophenazasiline (**5**) (37 mg, 0.10 mmol) in C_7D_8 (~ 0.25 mL) was added a cooled solution of $(\text{Ph}_3\text{P})_2\text{Pt}(\eta^2\text{-C}_2\text{H}_4)$ (**6**) (75 mg, 0.10 mmol) in C_7D_8 (~ 0.50 mL) at 195 K. The tube was shaken to mix the contents and then placed in a precooled NMR magnet at 223 K. Some gas evolution was observed in the dark reddish-brown reaction solution. NMR experiments were begun within 5 min of mixing.**

Selected NMR Data Collected 5 min after Mixing. ^1H NMR (500 MHz, C_7D_8 , 223 K): δ 5.74 (br s, unassigned), 5.29 (s, C_2H_4), 4.9 (m, unassigned), 4.80 (br s, unreacted **5**), 4.65 (m, SiH for **28**), 4.56 (s, H_2), 2.71 (s, C_2H_4 for **6**), -1.77 (dd, $^1J_{\text{PtH}} = 973$ Hz, $^2J_{\text{PH}} = 156$ (trans), 18 (cis), PtH for **28**). $^{31}\text{P}\{\text{H}\}$ NMR (202 MHz, C_7D_8 , 223 K): δ 35.5 (d, minor component, unassigned), 35.0 (br s, $^1J_{\text{PtP}} = 1863$, P trans to Si for **28**), 33.9 (s, minor component, **6**), 33.6 (br s, $^1J_{\text{PtP}} = 2417$, P trans to H for **28**), 25.4 (s, OPPh_3). The ^1H and $^{31}\text{P}\{\text{H}\}$ NMR spectra remained essentially the same after 2 h at 223 K except the signals for **6** were no longer observed.

Selected NMR Data Collected 3–4 h after Mixing. $^{31}\text{P}\{\text{H}\}$ NMR (202 MHz, C_7D_8 , 243 K): δ 34.8 (br s, $^1J_{\text{PtP}} = 1860$, **28**), 33.8 (br s, $^1J_{\text{PtP}} = 2421$, **28**), 25.3 (s, OPPh_3). ^1H NMR (500 MHz, C_7D_8 , 243 K): δ 5.28 (s, C_2H_4), 4.9 (br, minor component, unassigned), 4.63 (br m, SiH for **28**), 4.54 (s, H_2), -1.85 (br d, $^1J_{\text{PtH}} = 969$, $^2J_{\text{PH}} = 146$, PtH for **28**).

Selected NMR Data Collected 5 h after Mixing. ^1H NMR (500 MHz, C_7D_8 , 263 K): δ 5.27 (s, C_2H_4), 4.63 (br m, SiH for **28**), 4.48 (s, minor component, H_2), -1.92 (br d, $^1J_{\text{PtH}} = 968$, $^2J_{\text{PH}} = 149$, PtH for **28**). $^{31}\text{P}\{\text{H}\}$ NMR (202 MHz, C_7D_8 , 263 K): δ 34.4 (br, $^1J_{\text{PtP}} = 1858$, **28**), 33.9 (s, $^1J_{\text{PtP}} = 2424$, **28**), 24.8 (s, OPPh_3).

Selected NMR Data Collected 6 h after Mixing. ^1H NMR (500 MHz, C_7D_8 , 283 K): δ 5.26 (br s, C_2H_4), 4.63 (m, SiH for **28**), 4.51 (s, H_2), -1.98 (br s, $^1J_{\text{PtH}} = 962$, PtH for **28**). $^{31}\text{P}\{\text{H}\}$ NMR (202 MHz, C_7D_8 , 283 K): δ 5–45 (br), 24.6 (s, OPPh_3).

Selected NMR Data Collected 7 h after Mixing. The ^1H NMR spectrum did not exhibit any hydride signals for **28** or any other complexes. $^{31}\text{P}\{\text{H}\}$ NMR (202 MHz, C_7D_8 , 303 K): δ 22 (br, range 5–45 ppm), 24.4 (s, OPPh_3). Several minor unassigned resonances appeared between 10 and 35 ppm.

Selected NMR Data Collected 22 h after Mixing. $^{31}\text{P}\{\text{H}\}$ NMR (202 MHz, C_7D_8 , 303 K): δ 66.2 (s, minor component, **31**), 29.8 (s, minor component, unassigned), 28.4 (s, $^1J_{\text{PtP}} = 1682$ Hz, **29**), 24.8 (s, minor component, unassigned), 24.5 (s, OPPh_3). ^1H NMR (500 MHz, C_7D_8 , 223 K): δ 4.6 (s, H_2), 2.91 (d, $^2J_{\text{PH}} = 11$, $\text{Pt}\cdots\text{H}\cdots\text{Si}$) for **30**), -6.35 (br t, Pt–H for **30**). $^{31}\text{P}\{\text{H}\}$ NMR (202 MHz, C_7D_8 , 223 K): δ 65.1 (s, minor component, **31**), 28.2 (s, **29**), 26.8 (t, PtPPh_3 for **30**), 25.5 (s, OPPh_3), 18.6 (d, $\text{Pt}(\text{PPh}_3)_2$ for **30**), -6.6 (br s, PPh_3).

After approximately one week, orange X-ray-quality crystals were recovered from the reaction solution upon decanting the orange, soluble fraction. The orange solid **30** cocrystallized with three C_7D_8 solvent molecules.

Selected NMR Data for the Soluble Fraction after Removal of Crystalline Solid (30**) after ca. 3 weeks.** $^{31}\text{P}\{\text{H}\}$ NMR (202 MHz, C_7D_8 , 190 K): 28.1 (br s, minor component, **29**), 25.4 (s, OPPh_3), 10.2 (s, $^1J_{\text{PtP}} = 3831$, major component, $\text{Pt}(\text{PPh}_3)_4$), -7.9 (s, major component, PPh_3).

b. Room-Temperature Reaction. In an inert atmosphere drybox, a solution containing 2,8-dibromo-5-methyl-10,10-dihydrophenazasiline (**5**) (16 mg, 0.043 mmol) in C_7D_8 (0.75 mL) was added to

a vial containing $(\text{Ph}_3\text{P})_2\text{Pt}(\eta^2\text{-C}_2\text{H}_4)$ (**6**) (32 mg, 0.043 mmol). Gas evolution was observed immediately upon addition. The red-brown solution was then transferred to an NMR tube, and NMR experiments were begun within 15 min of initial mixing. Similar results were obtained when $\text{Pt}(\text{PPh}_3)_4$ was used as the precursor.

Selected NMR Data Collected 15 min after Mixing. ^1H NMR (500 MHz, C_7D_8 , 300 K): δ 5.25 (br s, C_2H_4), 4.86 (m, minor component, unassigned), 4.64 (br m, Si–H for **28**), 4.51 (s, H_2), -2.06 (br s, $^1J_{\text{Pt-P}} = 968$ Hz, PtH for **28**). $^{31}\text{P}\{\text{H}\}$ NMR (202 MHz, C_7D_8 , 300 K): δ 36.3 (s, minor component), 34.1 (s, minor component), 29.7 (s, minor component), 27 (br, range 0–50 ppm), 25.8 (s, OPPh_3).

Selected NMR Data Collected 45 min after Mixing. ^1H NMR (500 MHz, C_7D_8 , 223 K): δ 5.29 (s, C_2H_4), 4.64 (br, SiH for **28**), 4.55 (s, H_2), -1.82 (br, PtH for **28**), -6.35 (t, PtH for **30**), $\text{Pt}\cdots\text{H}\cdots\text{Si}$ resonance not resolved. $^{31}\text{P}\{\text{H}\}$ NMR (202 MHz, C_7D_8 , 223 K): δ 74.5 (s, minor component, **31**), 28.0 (t, PtPPh_3 for **30**), 26.7 (s, OPPh_3), 20.0 (d, $\text{Pt}(\text{PPh}_3)_2$ for **30**), -5.0 (br, PPh_3), several minor resonances were observed between 18 and 40 ppm.

In a similar experiment run at room temperature, a solution containing 2,8-dibromo-5-methyl-10,10-dihydrophenazasiline (**5**) (39 mg, 0.11 mmol) in C_7D_8 (1.0 mL) was reacted with $(\text{Ph}_3\text{P})_2\text{-Pt}(\eta^2\text{-C}_2\text{H}_4)$ (**6**) (76 mg, 0.10 mmol). Within 24 h an orange crystalline solid, **30**, was obtained (56 mg, 51% based on $30\cdot 3\text{C}_7\text{D}_8$). NMR data for complex **30**: ^1H NMR (500 MHz, C_7D_8 , 223 K): δ 8.1–6.0 (ArH), 2.91 (d, $^1J_{\text{PtH}}$ not resolved, $^2J_{\text{PH}} = 11$, $\text{Pt}\cdots\text{H}\cdots\text{Si}$), 2.58 (s, NMe), 2.41 (s, NMe), -6.34 (t, $^1J_{\text{PtH}} = 564$, $^2J_{\text{PH}} = 15$, PtH). $^{31}\text{P}\{\text{H}\}$ NMR (202 MHz, C_7D_8 , 223 K): δ 28.1 (t, $^1J_{\text{PtP}} = 4032$, $^2J_{\text{PP}} = 280$, $^3J_{\text{PP}} = 28$, PtPPh_3), 18.5 (d, $^1J_{\text{PtP}} = 3710$, $^2J_{\text{PP}}$ not resolved, $\text{Pt}(\text{PPh}_3)_2$). $^{31}\text{P}\text{-}^{31}\text{P}\{\text{H}\}$ COSY NMR (202 MHz, C_7D_8 , 223 K): correlation between δ 28.1 (t) and 18.5 (d). $^1\text{H}\text{-}^{31}\text{P}$ COSY NMR (500 MHz, C_7D_8 , 223 K): correlation between δ 2.91 (d, $\text{Pt}\cdots\text{H}\cdots\text{Si}$) and 28.1 (t, PtPPh_3); correlation between δ -6.35 (t, PtH) and 18.5 (d, $\text{Pt}(\text{PPh}_3)_2$). $^1\text{H}\text{-}^{29}\text{Si}$ HMQC NMR (500 MHz, C_7D_8 , 223 K): correlation between δ 2.91 (d) and 136; correlation between δ -6.35 (t, PtH) and 137. IR (solid) (ν , cm^{-1}): 2276 (Pt–H), 1798 ($\text{Pt}\cdots\text{H}\cdots\text{Si}$). Anal. Calcd for $\text{C}_{80}\text{H}_{65}\text{-Br}_4\text{N}_2\text{P}_3\text{Pt}_2\text{Si}_2\cdot 3\text{C}_7\text{D}_8$: C, 54.79; H, 5.14. Found: C, 54.03; H, 3.94.

X-ray Structure Determinations. X-ray-quality crystals of **16**, **22**, and **30** were obtained from a C_7D_8 solution. Crystals with approximate dimensions $0.19 \times 0.10 \times 0.06$ units (**16**), $0.17 \times 0.10 \times 0.08$ units (**22**), and $0.24 \times 0.22 \times 0.20$ units (**30**) were mounted on glass fibers in a random orientation. Preliminary examination and data collection were performed using a Bruker SMART 1K charge coupled device (CCD) detector system single-crystal X-ray diffractometer using graphite-monochromated Mo $\text{K}\alpha$ radiation ($\lambda = 0.71073$ Å) equipped with a sealed tube X-ray source at 120 K. Preliminary unit cell constants were determined with a set of 45 narrow frame (0.4° in ϖ) scans. Typical data sets consisted of 3636 frames with a frame width of 0.3° in ϖ and typical counting time of 15–30 s/frame at a crystal-to-detector distance of 4.930 cm. The double-pass method of scanning was used to exclude any noise. The collected frames were integrated using an orientation matrix determined from the narrow frame scans. SMART and SAINT software packages³² were used for data collection and data integration. Analysis of the integrated data did not show any decay. Final cell constants were determined by global refinement of xyz centroids. Collected data were corrected for systematic errors using SADABS³³ based on the Laue symmetry using equivalent reflections. Crystal data and intensity data collection parameters are provide in the Supporting Information.

Structure solution and refinement were carried out using the SHELXTL-PLUS software package.³⁴ The structures were solved

(32) SMART and SAINT; Bruker Analytical X-Ray: Madison, WI, 2002.

(33) Blessing, R. H. *Acta Crystallogr.* **1995**, *A51*, 33.

(34) Sheldrick, G. M. *SHELXTL-PLUS*; Bruker Analytical X-Ray Division: Madison, WI, 2002.

by direct methods and refined successfully in the monoclinic space group $P2_1/c$ (**30**) and the triclinic space group $P\bar{1}$ (**16** and **22**), respectively. Full matrix least-squares refinement was carried out by minimizing $\sum w(F_o^2 - F_c^2)^2$. All three crystals were found to be toluene- d_8 solvates (two and one-half C_7D_8 for **16**; one C_7D_8 for **22**; three C_7D_8 for **30**). The non-hydrogen atoms were refined anisotropically to convergence. The hydrides bound to Pt for structures **22** and **30** were located from the difference Fourier synthesis but could not be refined. All other hydrogen atoms were included in their calculated positions and treated using appropriate riding models (AFIX m3). The projection view of the molecules with non-hydrogen atoms are represented by 50% probability ellipsoids and show the atom labeling for the asymmetric unit. The final residual values and structure refinement parameters are listed in the Supporting Information. Complete listings of positional and

isotropic displacement coefficients for hydrogen atoms and anisotropic displacement coefficients for the non-hydrogen atoms are listed in the Supporting Information and are deposited with the Cambridge Crystallographic Data Center.

Acknowledgment. We are grateful for a grant from the National Science Foundation (CHE-0316023) for support of this work.

Supporting Information Available: Three CIF files containing X-ray crystallographic data for complexes **16**, **22**, and **30**. This material is available free of charge via the Internet at <http://pubs.acs.org>.

OM060391B